
Dipartimento di Fisica

Sapienza
Università di Roma


# Polarization issues for CMB devices


Observing the Universe with the Cosmic Microwave Background, 22-26 April 2014, L'Aquila, Dr. Daniele Buzi

# Outline

## Scientific target

- Cosmic Microwave Background Polarization

↓

**B modes**

## Experimental aspects

- QUBIC (Q & U Bolometric Interferometry for Cosmology) experiment
  - Shields analysis with GRASP

- Anti Reflection Structures (ARS)

# CMB Polarisation

Differently by CMB temperature anisotropy, the polarization is generated only by scattering; when we observe the polarization we are looking directly at the so-called last scattering surface (LSS) of the photons → direct probe of the Universe at the epoch of recombination

- CMB Polarisation is due to the Thomson scattering of the radiation pattern at the recombination

↓

To obtain a net linear polarized signal, a local temperature quadrupole anisotropy pattern in the primordial plasma is needed

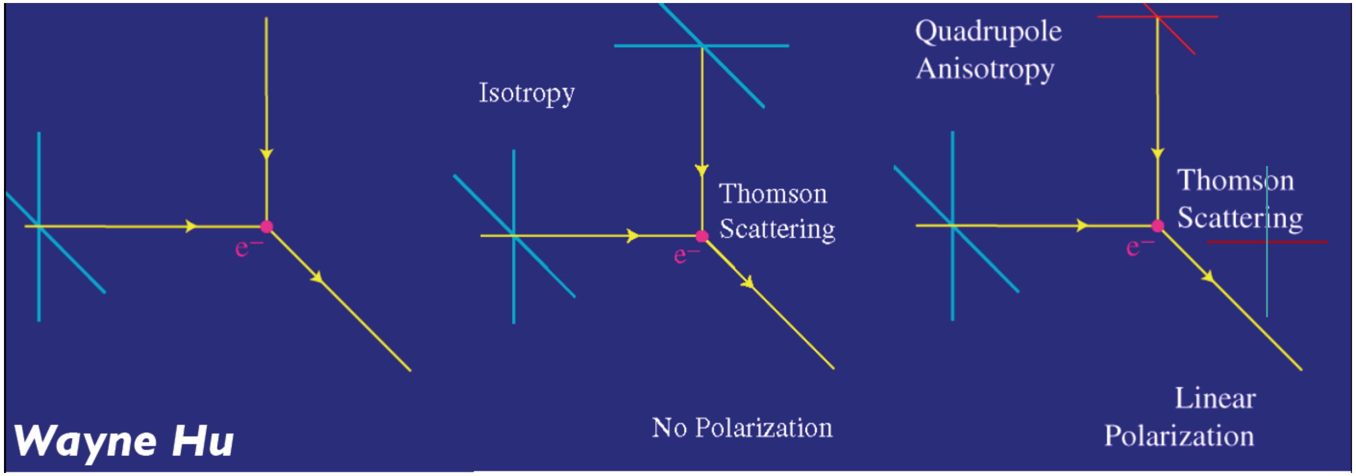


Only about 10 % of the CMB is polarized → few μK

# CMB Polarisation

3 Sources of the quadrupole temperature anisotropy @ recombination

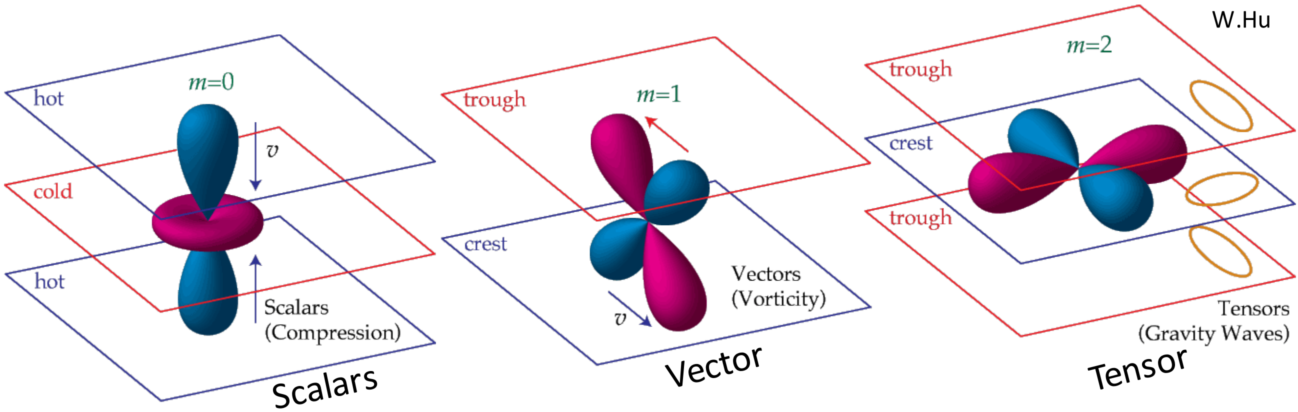


- Scalar Perturbations: density perturbations in the plasma → symmetric quadrupole
- Vector Perturbations: vorticity in the plasma (negligible @ recombination)
- Tensor Perturbations: due to gravitational waves that stretch and squeeze space and λ of the CMB photons → asymmetric quadrupole → polarization pattern "handedness"

# E and B modes

CMB polarisation sky pattern can be decomposed into 2 components

- ❑ E-mode ⟶ gradient component (even)
- ❑ B-mode ⟶ curl component (odd)

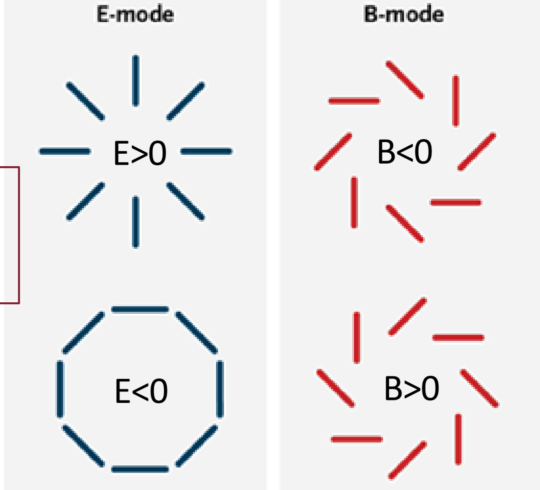


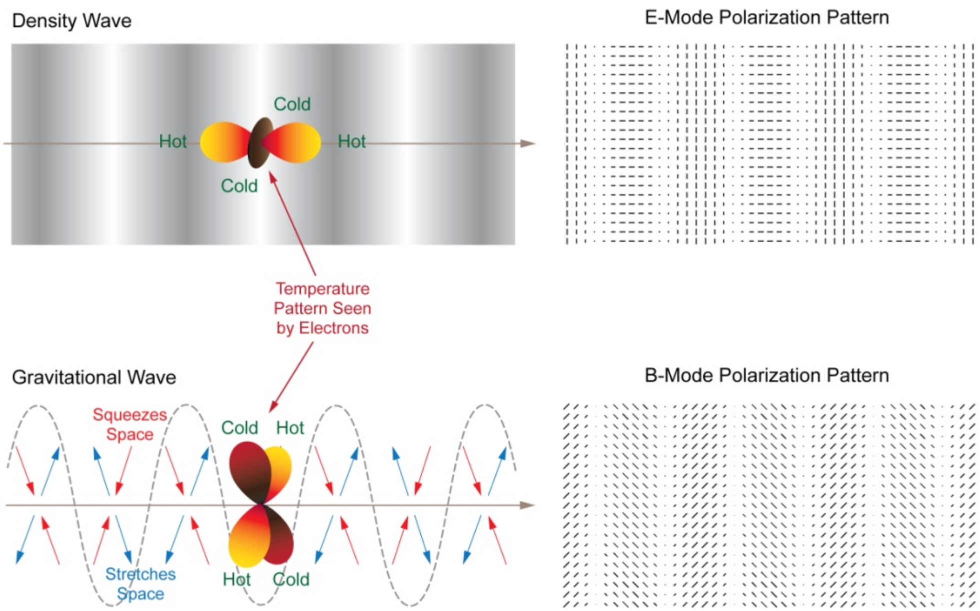


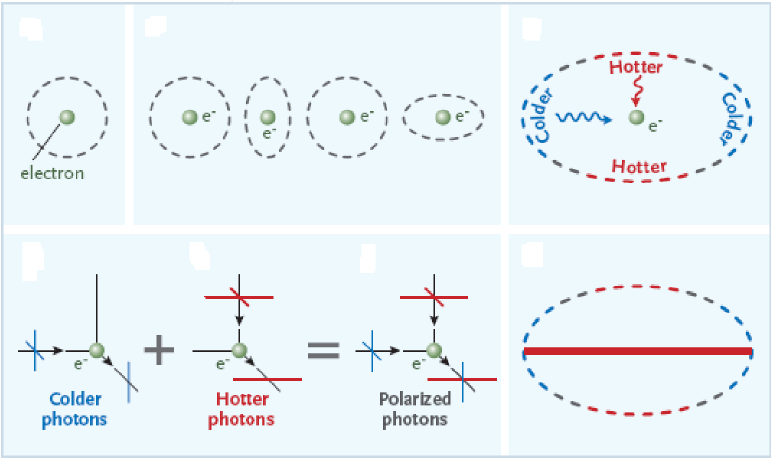

# CMB Polarisation

## Why we want to measure B modes?

$\zeta$ Scalar perturbations (density fluctuations) → only E modes

Fluctuations we observe today originated from quantum fluctuations generated during inflation

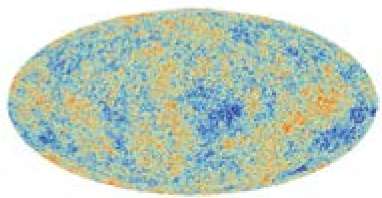

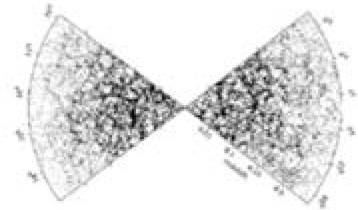

$h_{ij}$ Tensor perturbations (gravitational waves) → both E and B modes

Gravitational waves originated from quantum fluctuations generated during inflation

Detection of the B modes in CMB polarization pattern is the Holy Grail for Cosmology

**B modes are the smoking gun for Inflation theory** →

Measure of the tensor to scalar ratio at the energy scale of Inflation

$$\boxed{r_{ij} = \frac{h_{ij}}{\zeta}}$$

$$V^{\frac{1}{4}} = 1.06 \times 10^{16} GeV \left(\frac{r_{ij}}{0.01}\right)^{\frac{1}{4}}$$

# Interferometer *vs* Imager

## Actual instrumental techniques to measure B modes

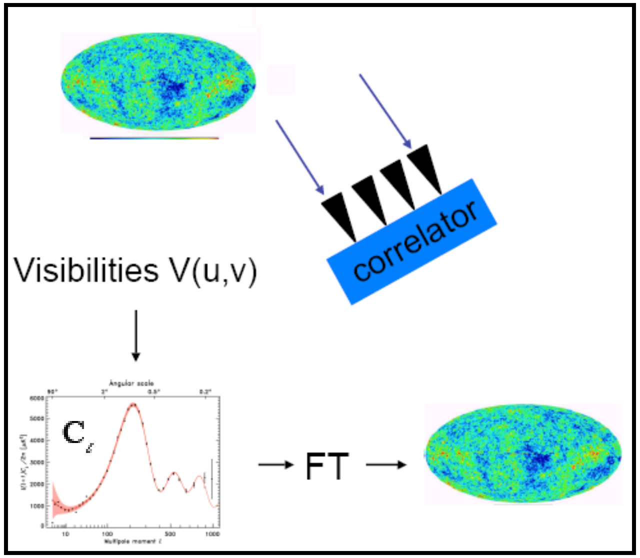


**vs**

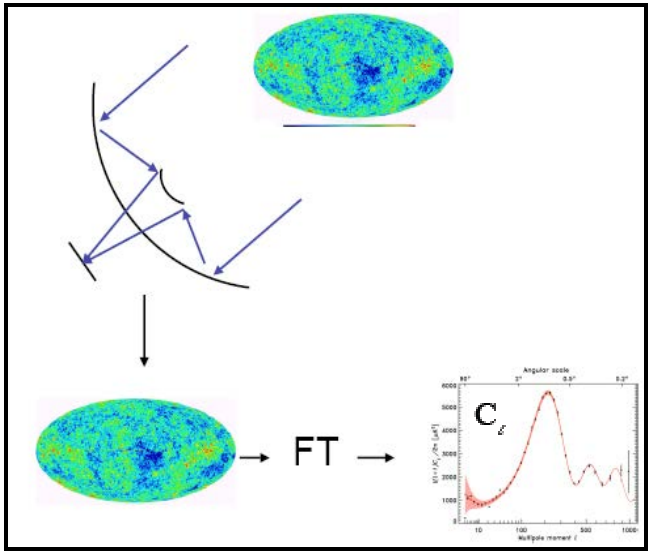


**INTERFEROMETERS**(CBI, DASI Interferometer)
- better control of the systematics
- no telescope → low ground pick-up and cross polarization
- angular resolution defined by antennas positions
- limited number of channels and amplifier noise

**IMAGERS** (BICEP, EBEX, SPIDER, QUITE, PolarBear)
- good sensitivity thanks to large bolometers arrays (wide band, low noise)
- systematics induced by telescope's presence
- angular resolution defined by antennas positions
- atmospheric noise → accurate scan strategy

# CMB Polarisation

A new technique that combines the advantages of the interferometers in terms of control of the systematics with high sensitivity of cryogenic bolometers

**BOLOMETRIC INTERFEROMETRY**

**Advantages**

**Comparable sensitivity as an imager:**

- same sky coverage
- # of detectors defined by # of baselines couples with same length and direction

**Direct measurement of the Fourier modes of all Stokes parameters:**

- direct measurement of E and B from interferometry

**High Sensitivity & Systematics are different:**

- use of low temperature bolometers (photon noise limited detectors)
- no mirrors → max collecting area
- reduction atmospheric contribution through interferometry

Measurement of the **Visibilities** that are the FT of the observed CMB sky field ($C_\ell$ CMB power spectrum is directly the square modulus of the visibilities)

Each bolometer measures the total power given by the sum of the radiation incoming from all antennas (Fizeau Interferometer) $<(E_1+E_2)^2>=<E_1{}^2>+<E_2{}^2>+2<E_1E_2{}^*>$

**Each bolometer measures linear combinations of all Stokes parameters I, Q and U**

# QUBIC

## Q & U Bolometric Interferometry for Cosmology

arXiv:
1010.0645
Astroparticle
Physics 34
(2011) 705-71

APC Paris, France
IAS Orsay, France
CSNSM Orsay, France
CESR Toulouse, France
Maynooth University, Ireland
Universita di Milano-Bicocca, Italy
Universita La Sapienza, Roma, Italy
University of Manchester, UK
Richmond University, USA
Brown University, USA
University of Wisconsin, USA

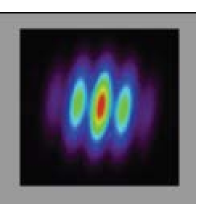

Constrain the B-modes down to r=0.01 @ 95% of confidence level

# QUBIC SITE: Dome C, Antarctica

Dome C site, Antarctica, is one of the best site for millimetre and sub-millimetre astronomy on Earth thanks to its low value of Precipitable Water Vapour (pwv)

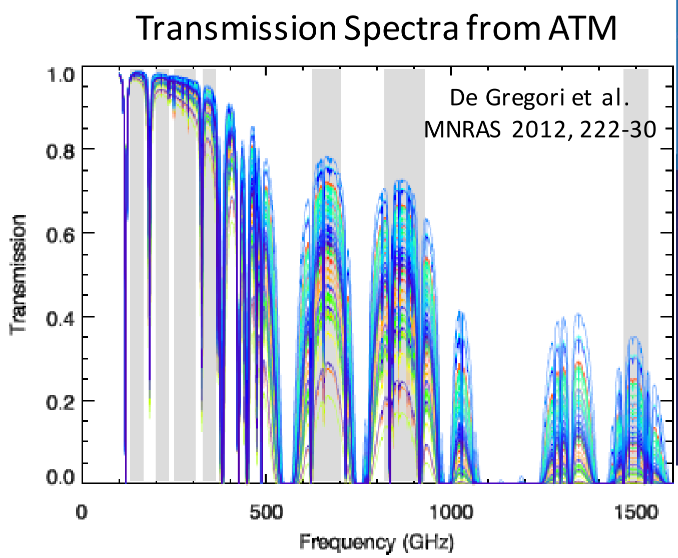


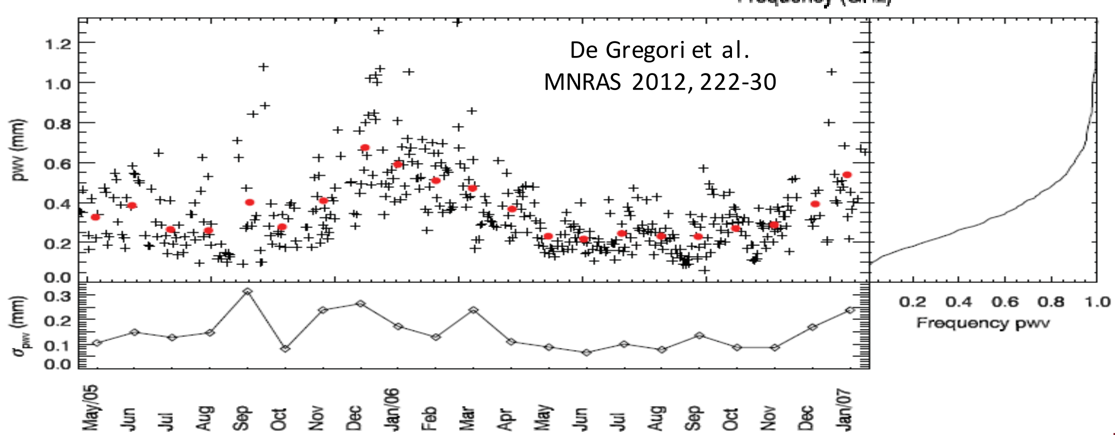


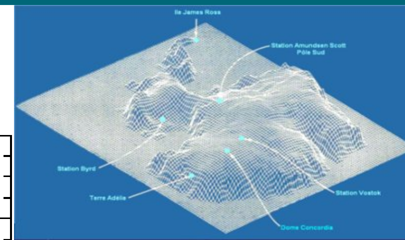


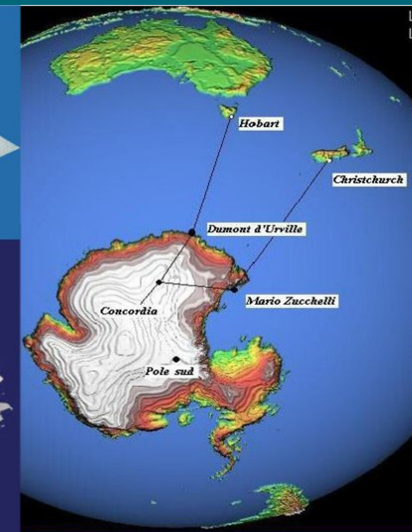


# QUBIC Analysis

Analysis relate to the necessity of shielding the QUBIC experiment in order to reduce unwanted radiation coming from different contamination sources

TICRA

The analysis has been realized with the support of the simulation software *GRASP* (General Reflector and Antenna Software Package) developed by TICRA Corp.

Goal of this analysis is the determination of the best geometrical configuration for the forebaffle and ground shield that should be installed in the QUBIC experiment

Study of the beam pattern of the instrument including sidelobes concerning spillover contributions

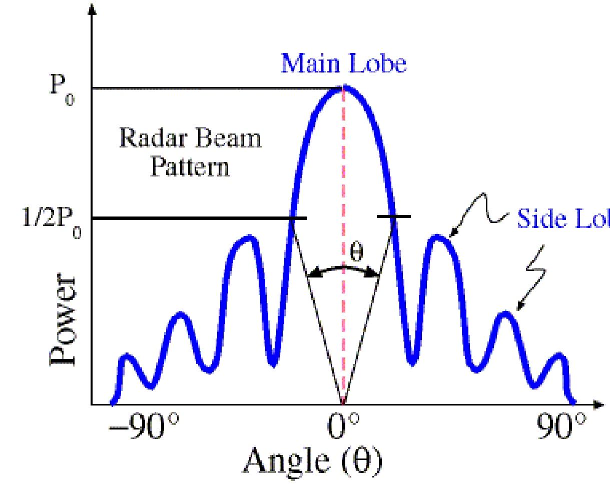


All the simulations have been performed using the MultiGTD approach (i.e. Geometric Theory of Diffraction ) suitable when the dimensions of the reflectors are thousandths times of wavelength

# QUBIC Beam

## Beam pattern analysis

Circular shape feed horn array
Feed horn array → 400 back to back (B2B) feed horns (total diameter = 300 mm)

**B2B feed horn array**

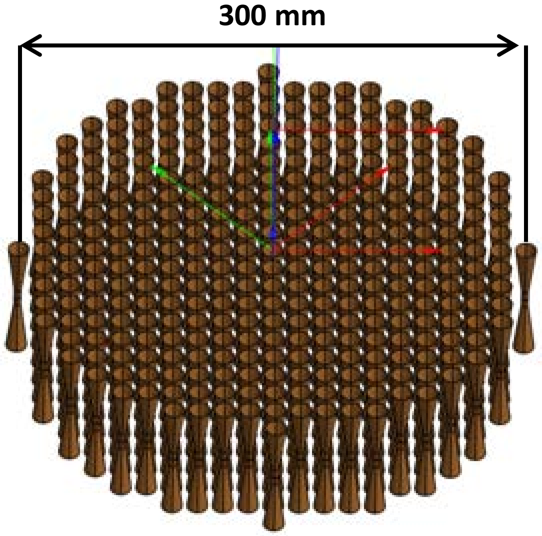


**Hybrid conical horn**

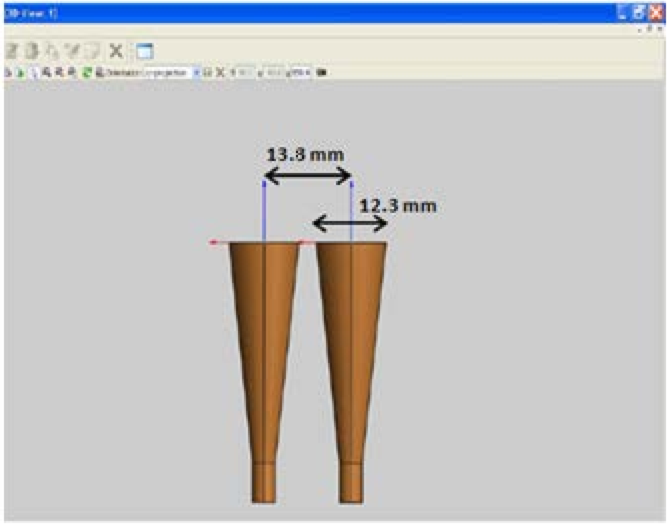


Each horn has been modelled with *GRASP* by a Hybrid Conical Horn with following parameters:

i. waveguide diameter = 4 mm
ii. horn diameter $d_h$ = 12.3 mm
iii. FWHM = 14 degrees
iv. centre to centre distance = 13.8 mm

# QUBIC Beam


Semi-flare angle α = 7°

All analysis has been performed @ λ = 150 GHz

**Single horn beam pattern**

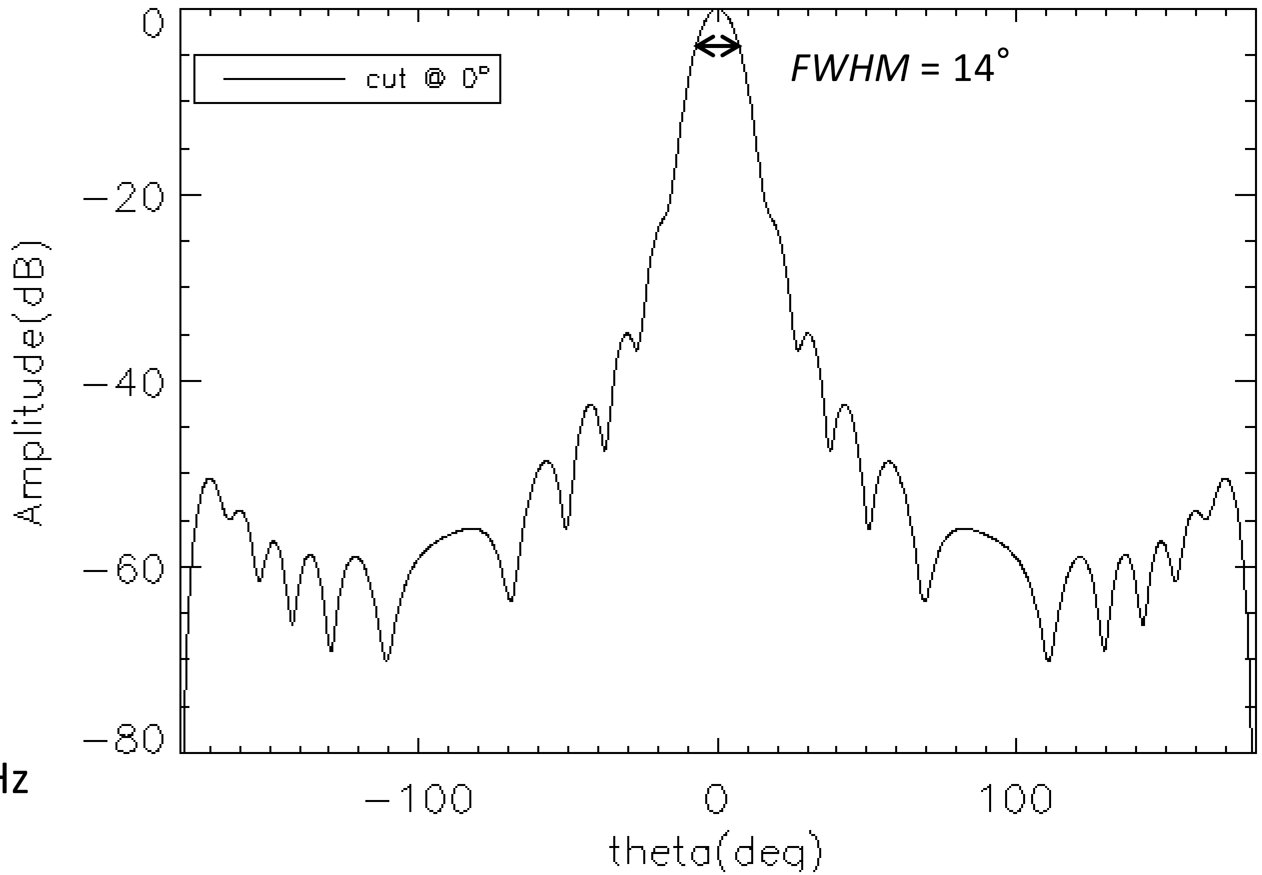

# QUBIC Beam

400 feed horns

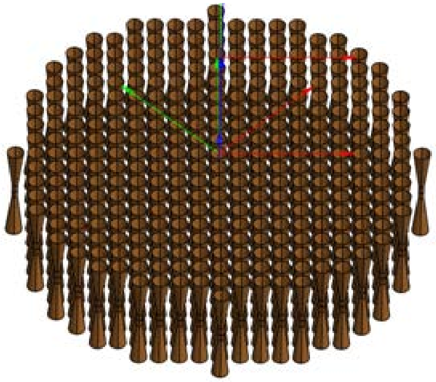

Synthesized beam pattern of the central pixel on the focal plane

max baseline $B_{max}$ = 300 mm
min baseline $B_{min}$ = 13.8 mm

Peaks angular distance: $\lambda / B_{max} = 0.57^{\circ}$
Peak angular size: $\lambda / B_{min} = 7.5^{\circ}$

**Synthesized beam**

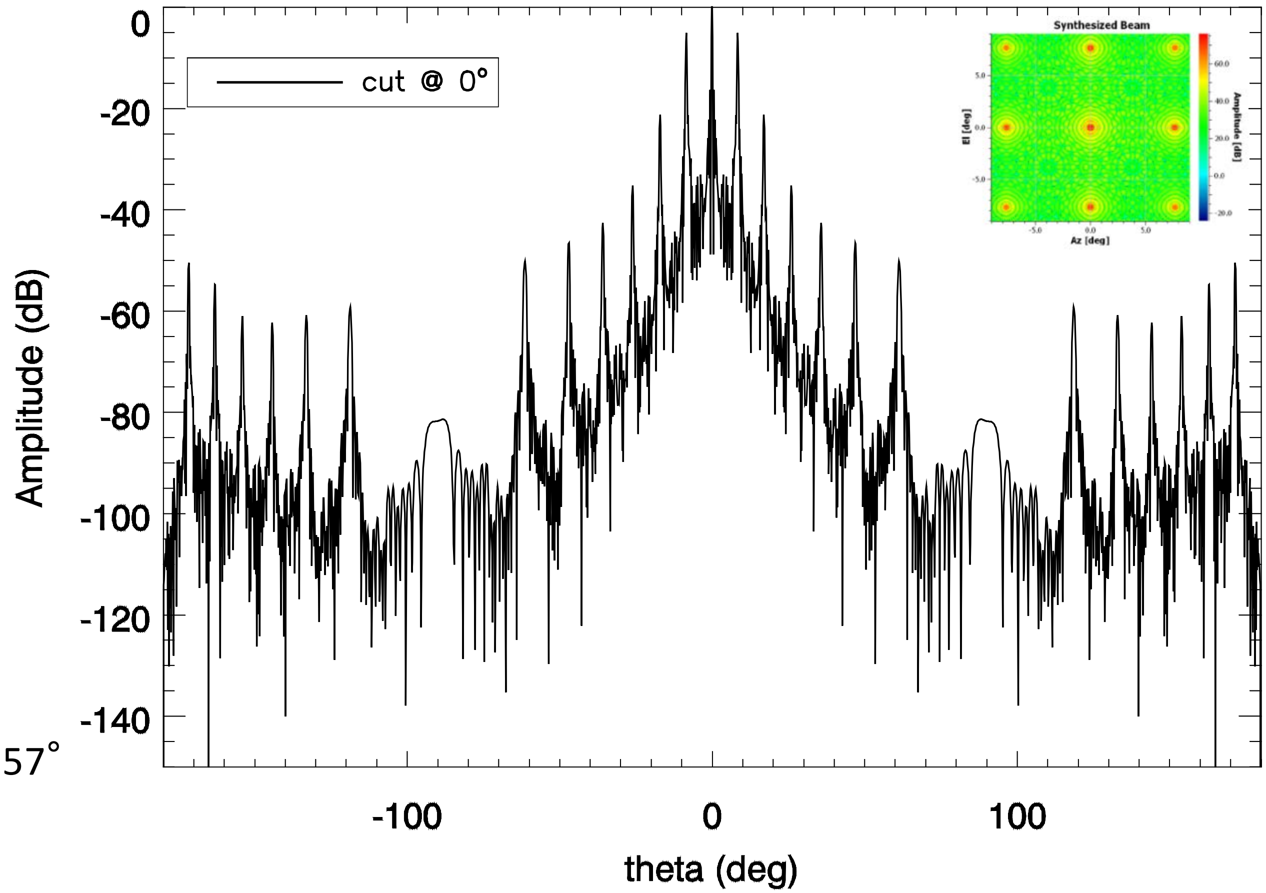

# QUBIC Shielding

In order to reduce spurious radiative contributions inside the QUBIC focal plane, have been investigated different solutions to correctly select the number and the geometry of the shields for the QUBIC experiment

## Forebaffle (FB)

- Fixed on cryostat’s window 100 mm above feed horn array
- Conical shape with aperture angle equal to 2*FWHM of single horn = 14°
- 350 mm base diameter and 500 mm height (TBD) has been investigated

Simulations have been performed considering reflective inner surface of the FB , other possible configurations are under investigation

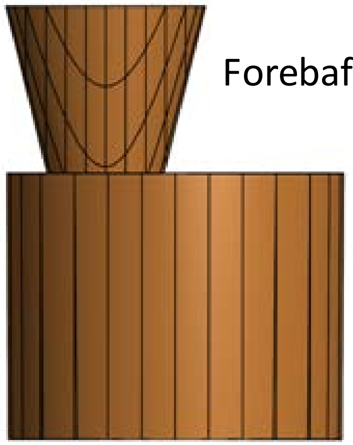

Forebaffle (FB)

QUBIC Cryostat

Shields inner surface

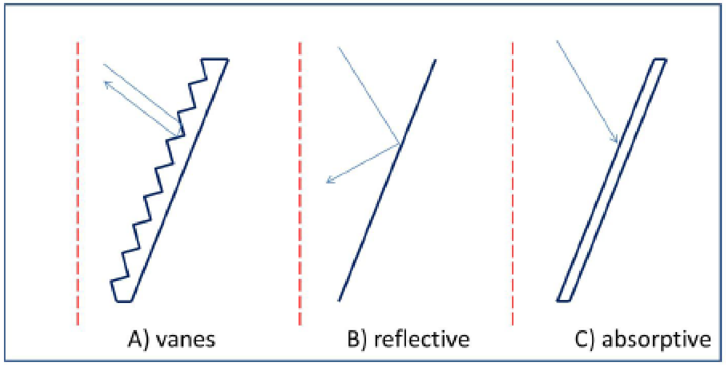


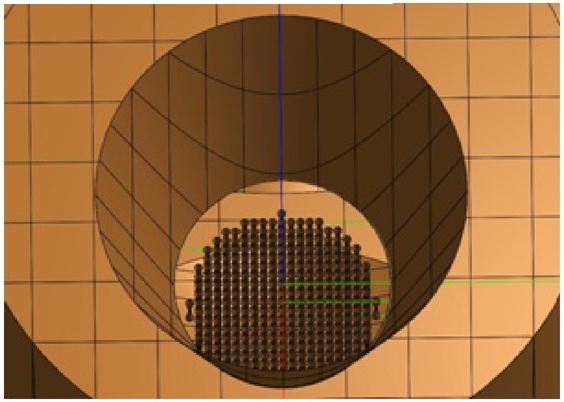

# QUBIC Shielding

Beam pattern of the central feed horn (cut @ 0 and 90 degrees) including or not the cryostat's window (no FB)

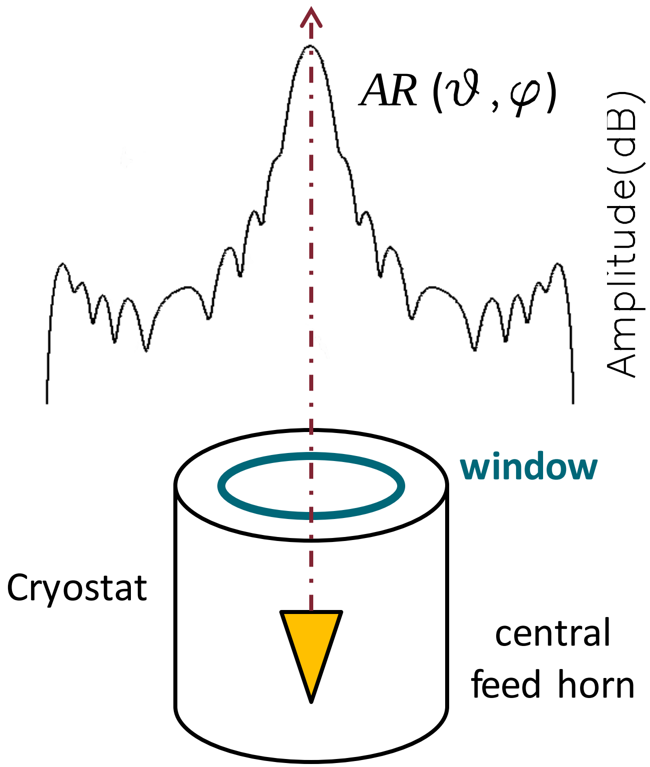


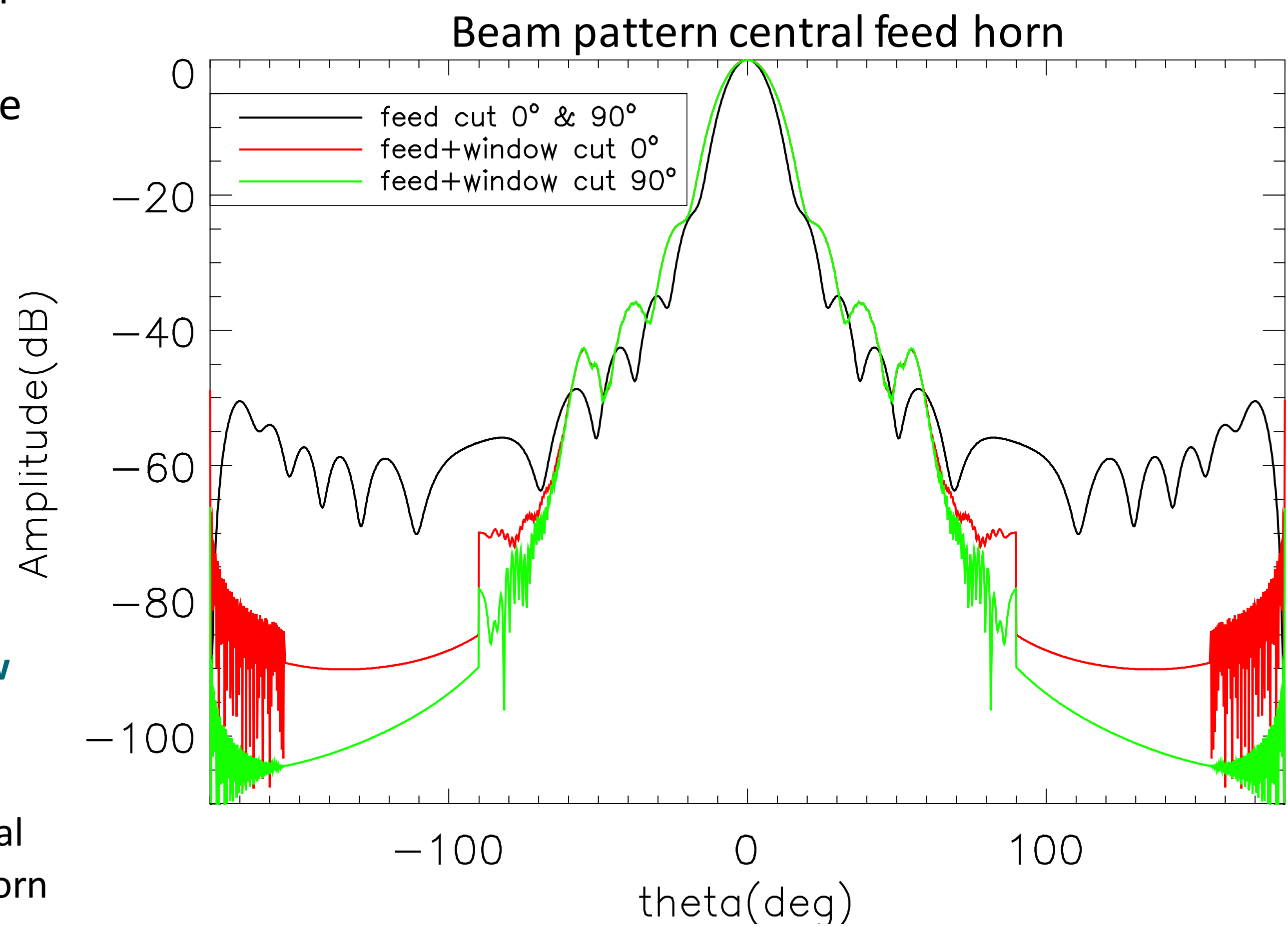

# QUBIC Shielding

Central feed horn beam pattern (cut @ 0 deg) with and without the presence of the FB

Including the FB the pattern shows/experiences a cut-off about at $\pm 20^\circ$ around the max

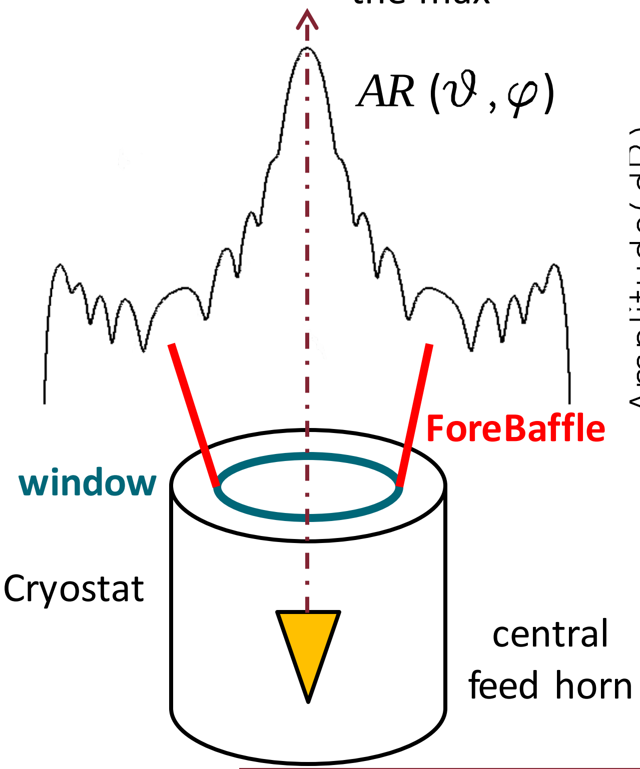


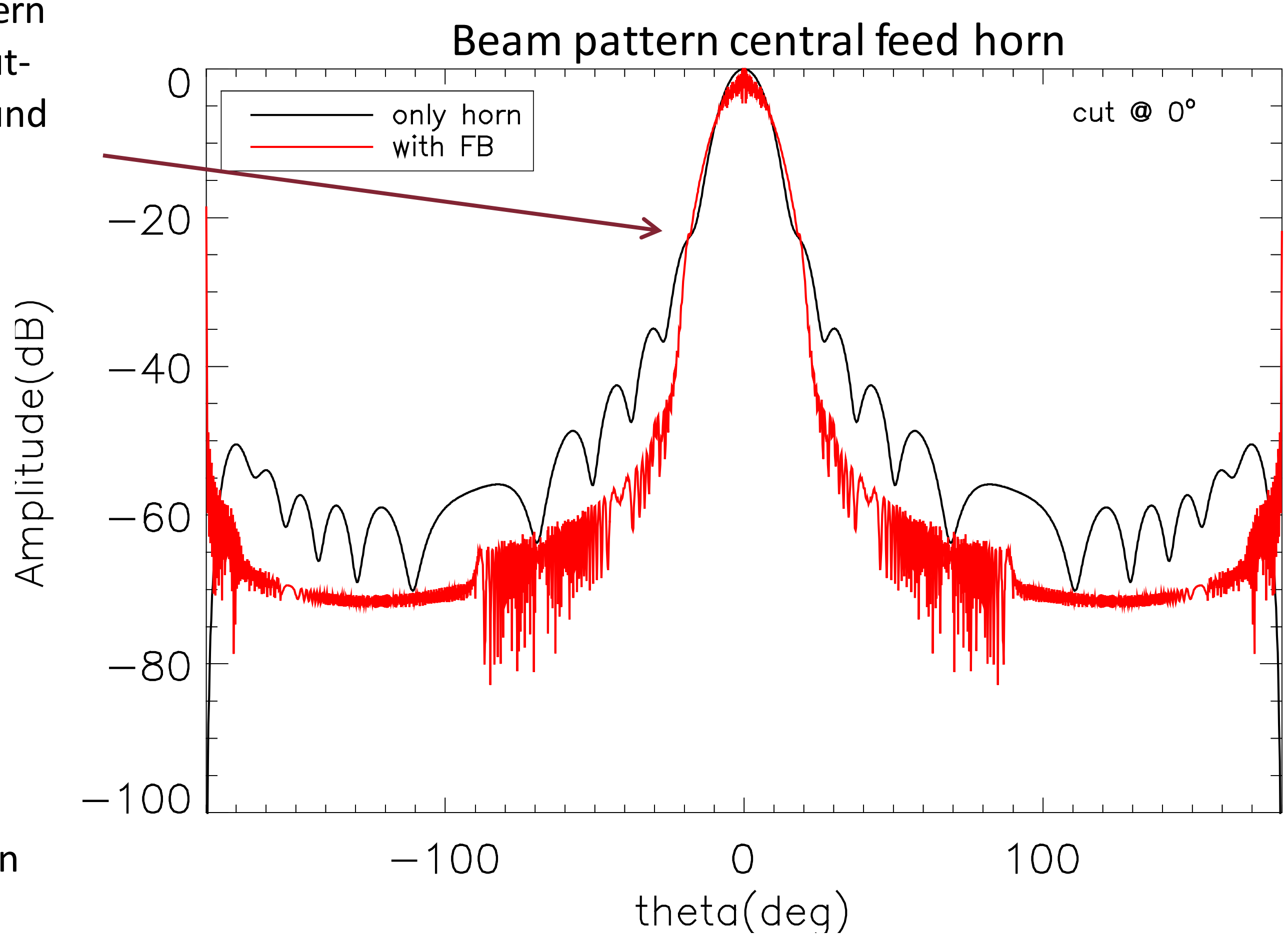

# QUBIC Shielding

Central feed horn beam pattern (cut @ 0 deg) for different FB heights (aperture angle = 14° )

Increasing FB height, the horn beam pattern experiences a cut-off a lower angles from boresight

**Increase the FB height over 1 meter is not useful**

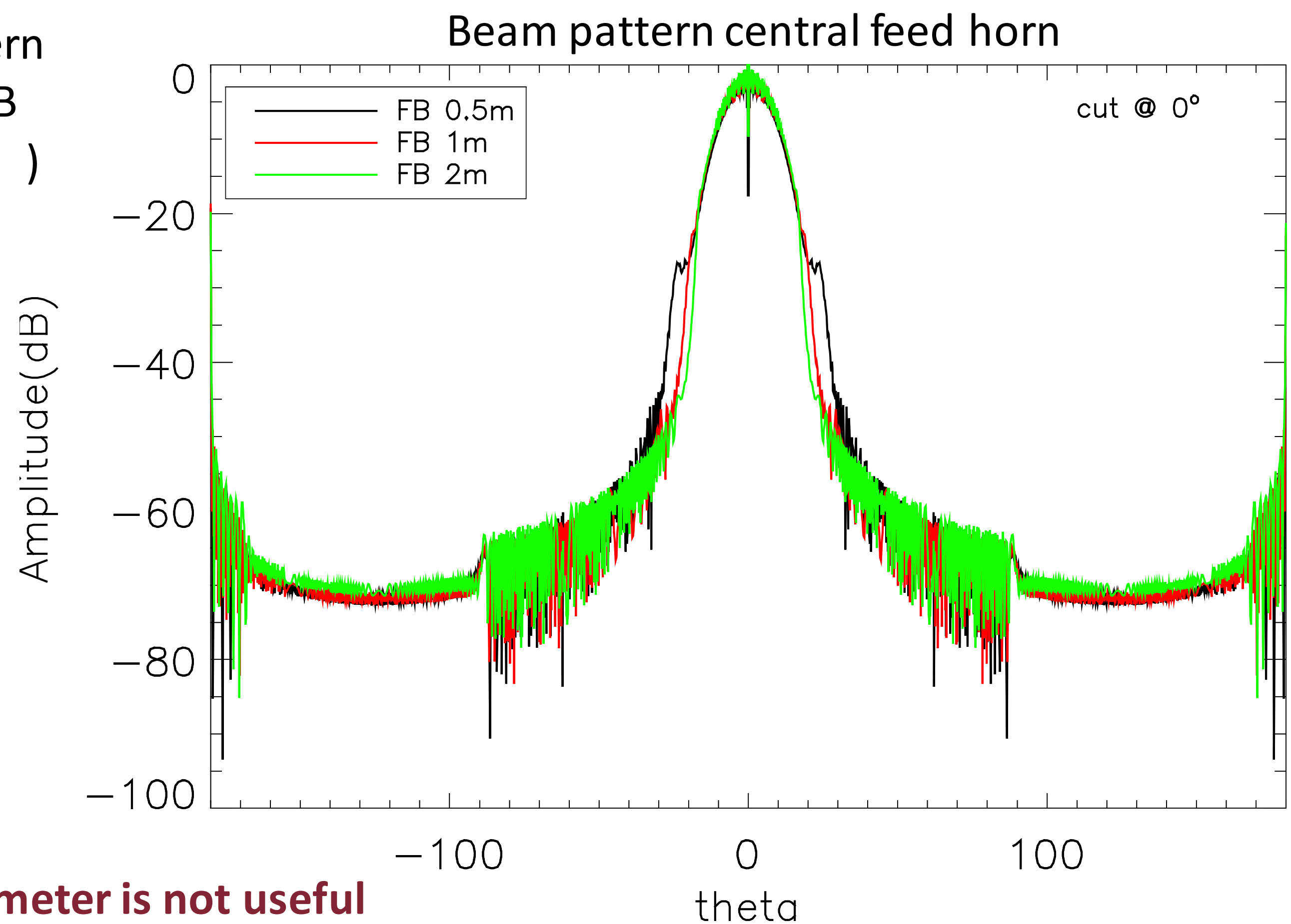

# QUBIC Shielding

Central feed horn beam pattern (cut @ 0 deg) obtained varying FB aperture angle (FB 1 meter height)

**14° aperture angle seems to be the good compromise**

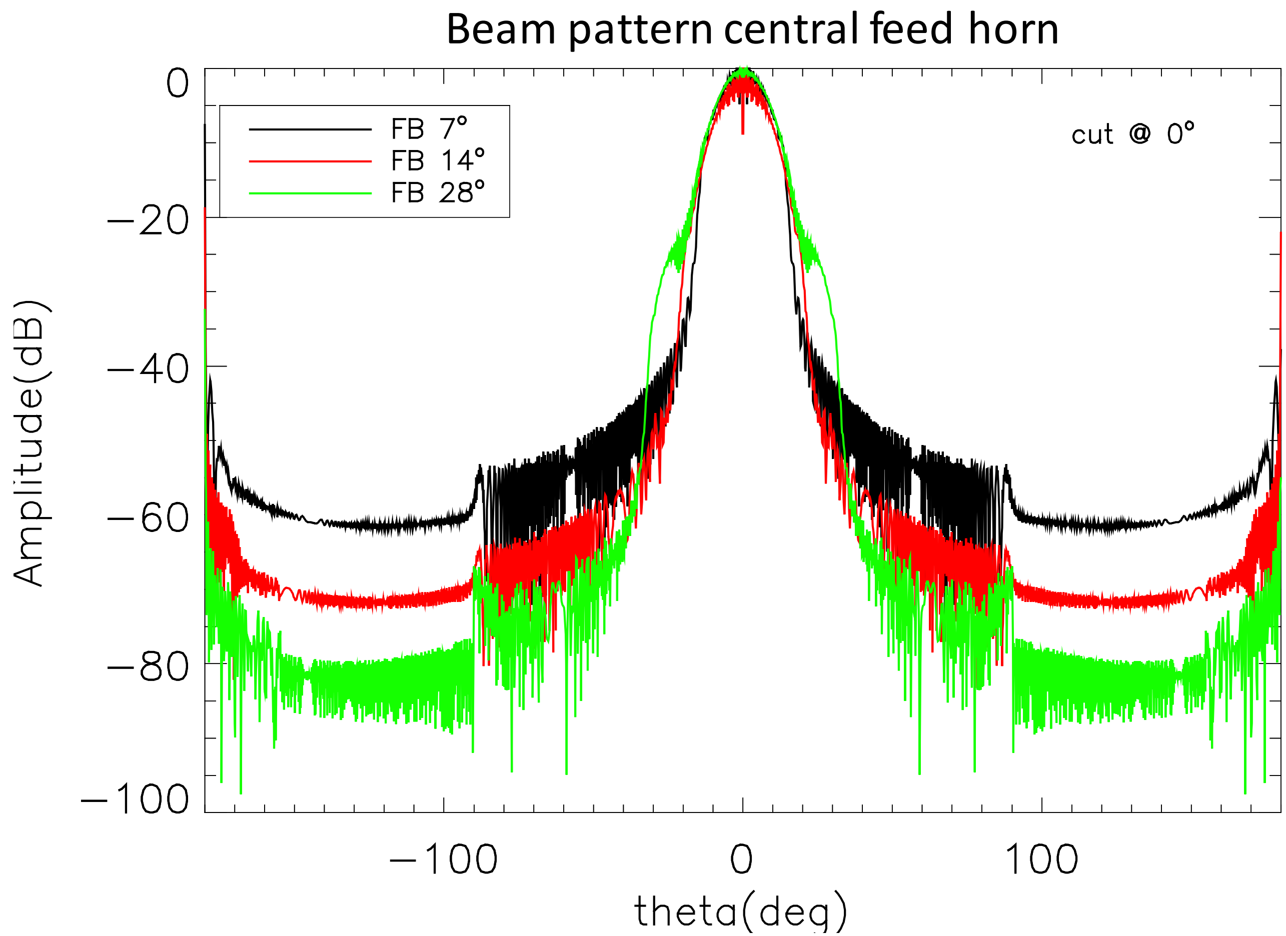

# QUBIC Shielding

In order to minimize the loading coming from the ground and picked up from the instrument, for QUBIC experiment has been planned the realization of a Ground Shield (GS) fixed on the ground

## Ground Shield (GS)

- Conical shape with aperture angle of 90°
- 3 m base diameter (TBD) placed 50 cm down the base instrument
- Fixed on the ground with a inner reflective surface

Ground shield (GS) 3D cad realized with GRASP

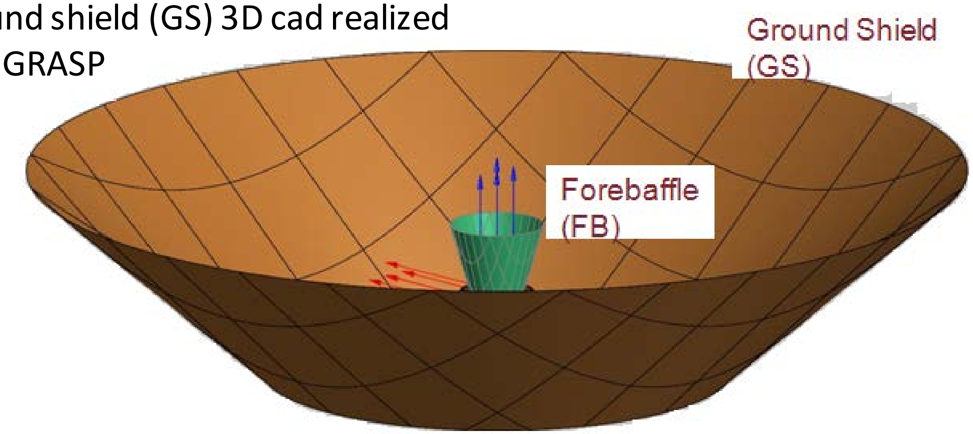


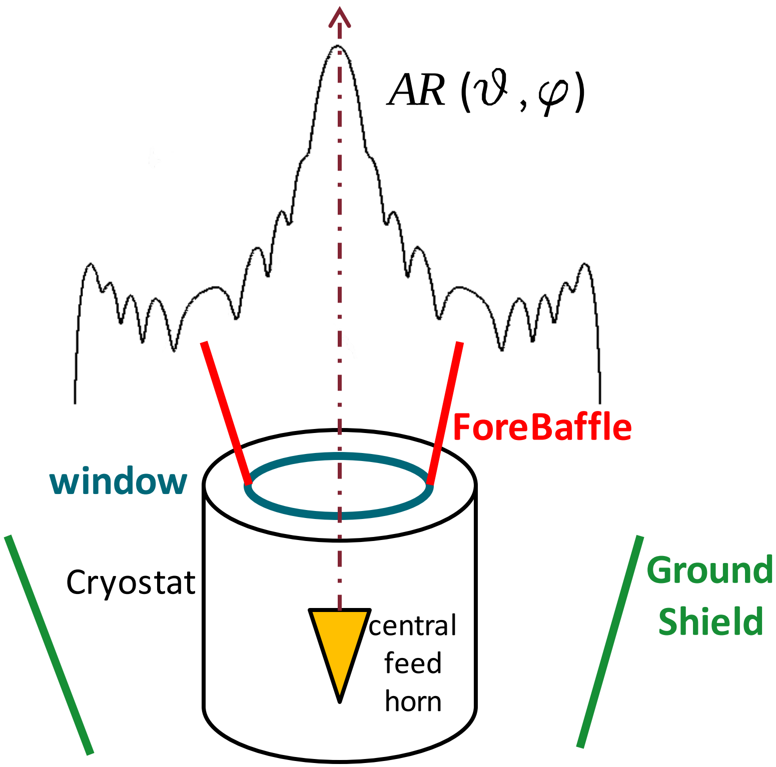

# QUBIC Shielding

Central feed horn beam pattern (spherical cuts @ 0 and 90 degrees) for the only FB and for the FB including GS at zenith position (i.e. varying the FB angular position inside the GS will have a different and asymmetric pattern)

The cuts-off (knees) experienced by the beam pattern at $\pm 90^{\circ}$ is given by the presence of the GS (the Grasp analysis has to be better modelled)

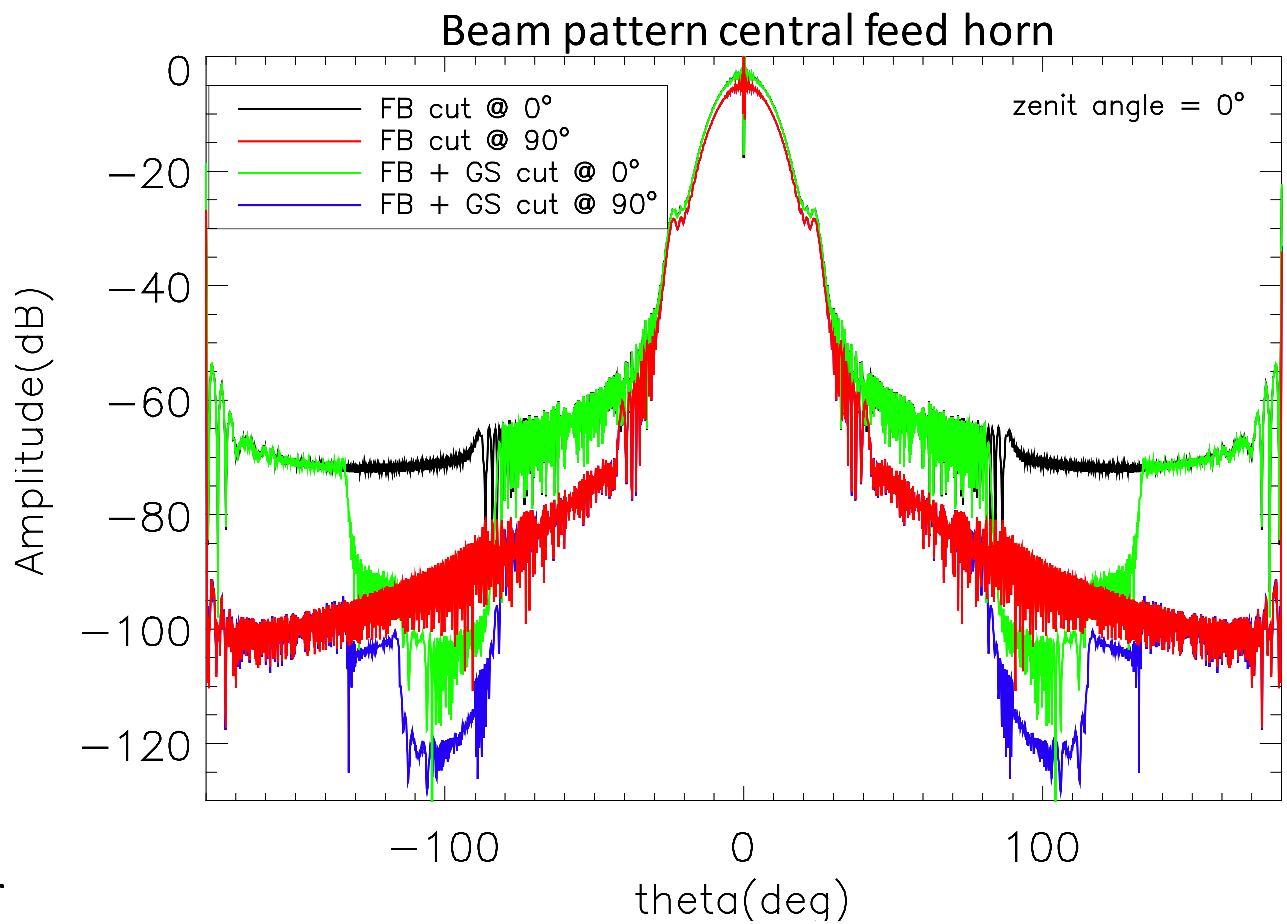

# QUBIC Shielding

Possibility to implement QUBIC shielding including a new shield in-built with the cryostat: Elizabethan Collar (EC) (i.e. in analogy with the veterinarian medical device)

**Elizabethan Collar (EC)**

- Conical shape with aperture angle of 28°
- 500 m base diameter (TBD) 100 mm up to the feed horn array
- Fixed on the cryostat with a inner reflective surface

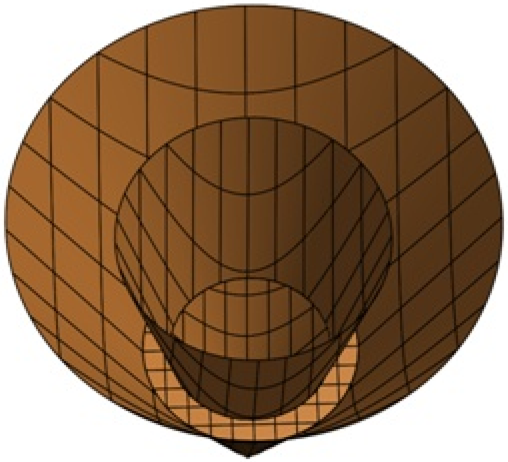

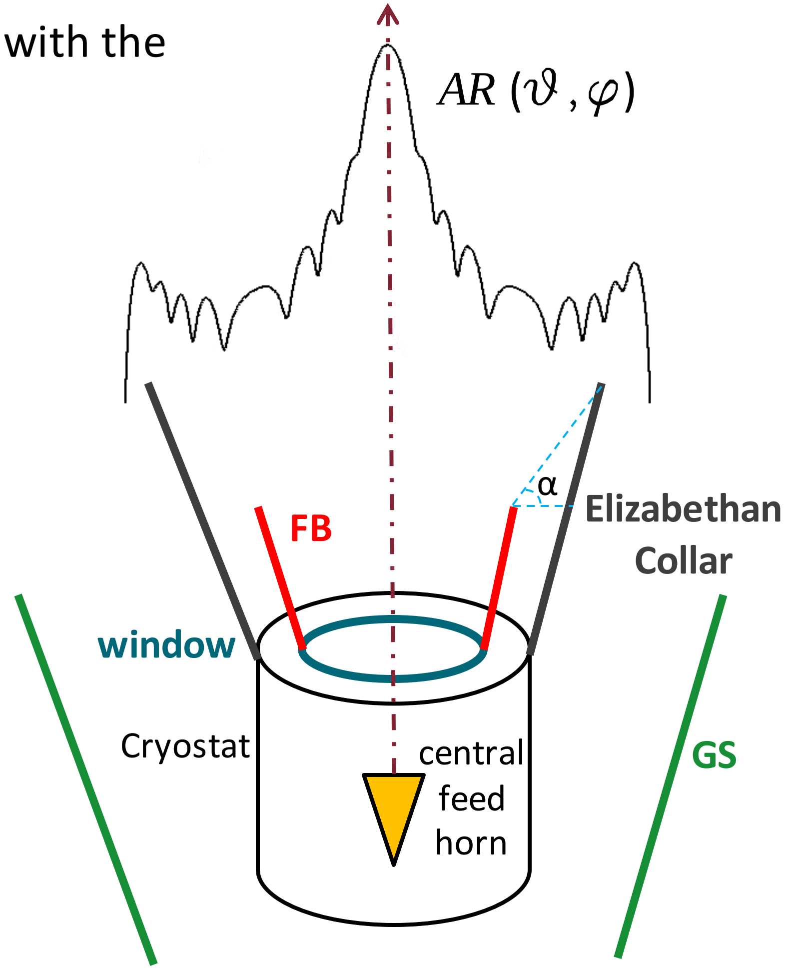

# QUBIC Shielding

Central feed horn beam pattern (spherical cut @ 0° ) obtained with the presence of the FB (0.5m height and aperture angle = 14° ) and of the EC for several values of α (different aperture angles and heights )

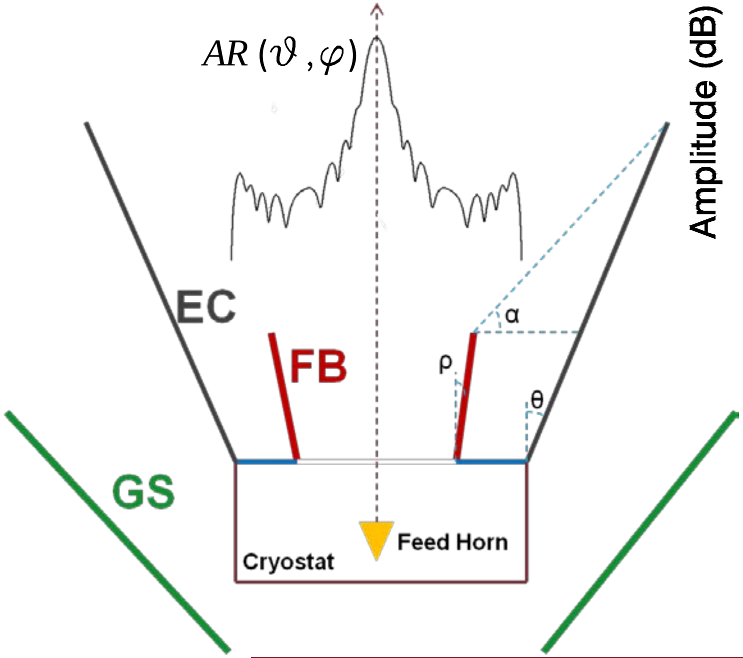


Beam pattern central feed horn

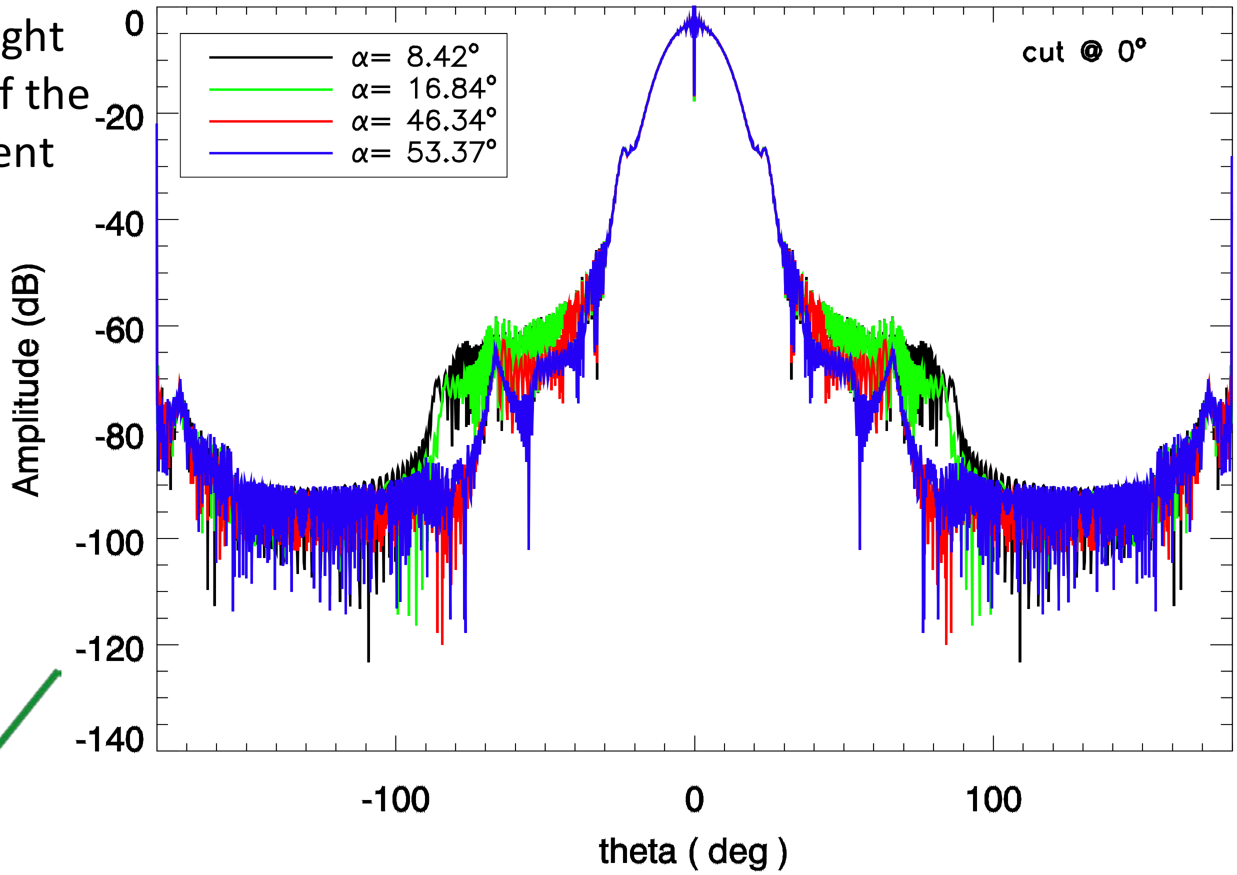

# QUBIC Spillover

Spillover contributions estimated for the 3 main contamination sources surrounding QUBIC experiment

Scan strategy: QUBIC will scan the sky from the zenith position to a minimum elevation equal to 35° (TBD), with an azimuth position diametrically opposite to the Sun and Moon

Evaluation of the spillover contributions on the entire detectors focal plane (efficiencies have not been included) in terms of temperature

$$S(z) = \frac{\int_{\Delta\theta}\int_{\Delta\phi} T(\theta,\phi) AR(\theta,\phi) sin\theta d\theta d\phi}{\int_{\Delta\theta}\int_{\Delta\phi} AR(\theta,\phi) sin\theta d\theta d\phi}$$

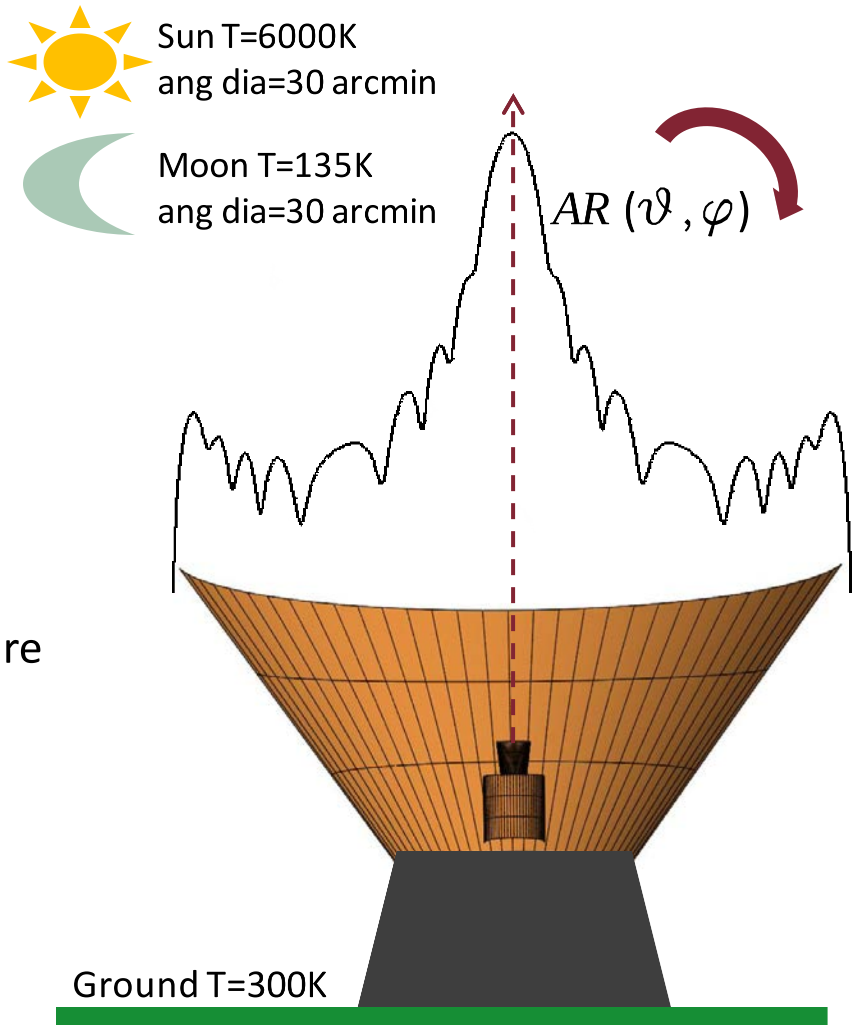

# QUBIC Spillover

Spillover evaluation related to the presence of the Ground (T=300K, emissivity=1)
Vertical line indicates the maximum zenithal angle reached during QUBIC sky scan (TBD)

**Black curve**: central feed horn main beam pattern (see slide 17)
**Red curve**: central feed horn beam pattern including FB (see slide 21)

Ground spillover @ zenithal position:

- 627 mK no FB
- 111 mK with FB

$$S(z) = \frac{\int_{\Delta\theta}\int_{\Delta\phi} T(\theta,\phi) AR(\theta,\phi) sin\theta d\theta d\phi}{\int_{\Delta\theta}\int_{\Delta\phi} AR(\theta,\phi) sin\theta d\theta d\phi}$$

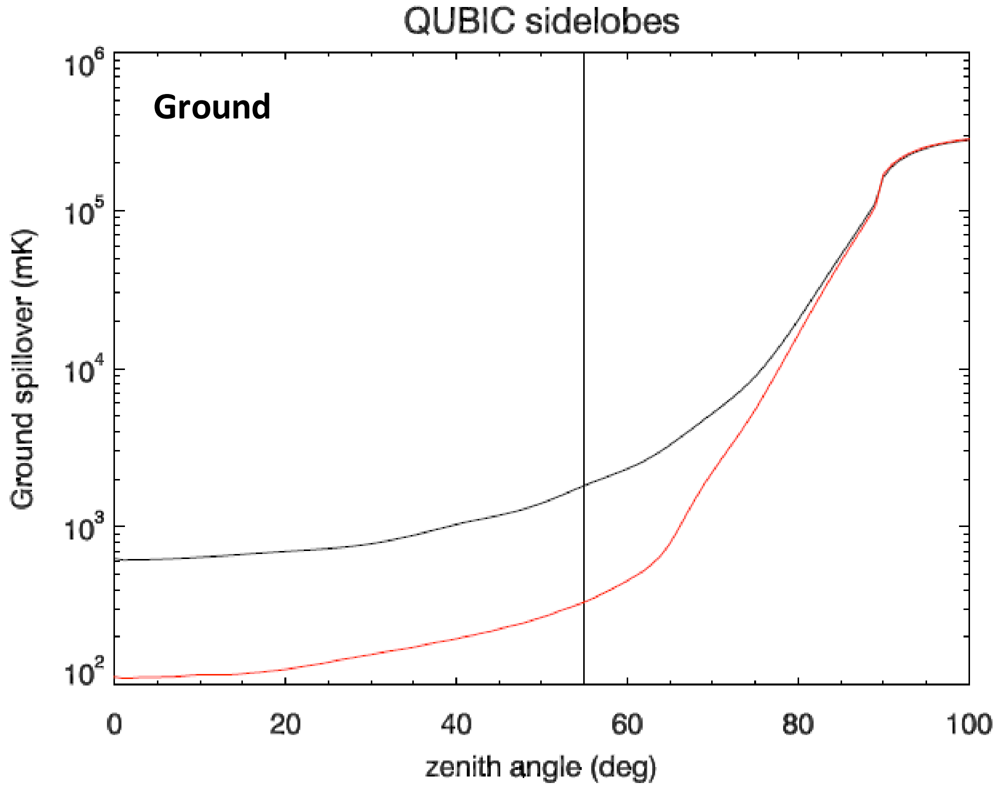

# QUBIC Spillover

Spillover evaluation related to the presence of the Sun (T=6000K, angular diameter = 30 arcmin), (@ horizon, opposite azimuth position)

$$S(z) = \frac{\int_{\Delta\theta}\int_{\Delta\phi} T(\theta,\phi) AR(\theta,\phi) sin\theta d\theta d\phi}{\int_{\Delta\theta}\int_{\Delta\phi} AR(\theta,\phi) sin\theta d\theta d\phi}$$

Vertical line indicates the maximum zenithal angle reached during QUBIC sky scan (TBD)

**Black curve**: central feed horn main beam pattern (see slide 17)

**Red curve**: central feed horn beam pattern including FB (see slide 21)

Ground spillover @ zenithal position:

- 3 mK no FB
- 328 μK with FB

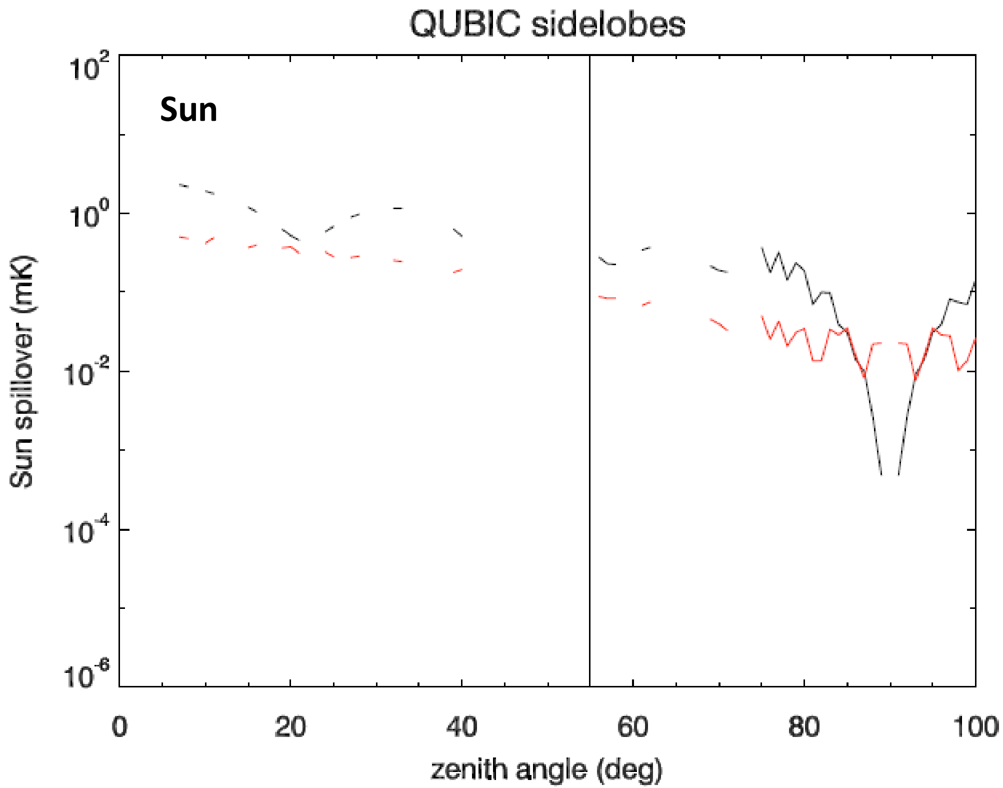

# QUBIC Spillover

Spillover evaluation related to the presence of the Sun (T=135K, angular diameter = 30 arcmin), (@ horizon, opposite azimuth position)

Vertical line indicates the maximum zenithal angle reached during QUBIC sky scan (TBD)

**Black curve**: central feed horn main beam pattern (see slide 17)
**Red curve**: central feed horn beam pattern including FB (see slide 21)

Ground spillover @ zenithal position:
- 70 μK no FB
- 111 μK with FB

$$S(z) = \frac{\int_{\Delta\theta}\int_{\Delta\phi} T(\theta,\phi)AR(\theta,\phi)sin\theta d\theta d\phi}{\int_{\Delta\theta}\int_{\Delta\phi} AR(\theta,\phi)sin\theta d\theta d\phi}$$

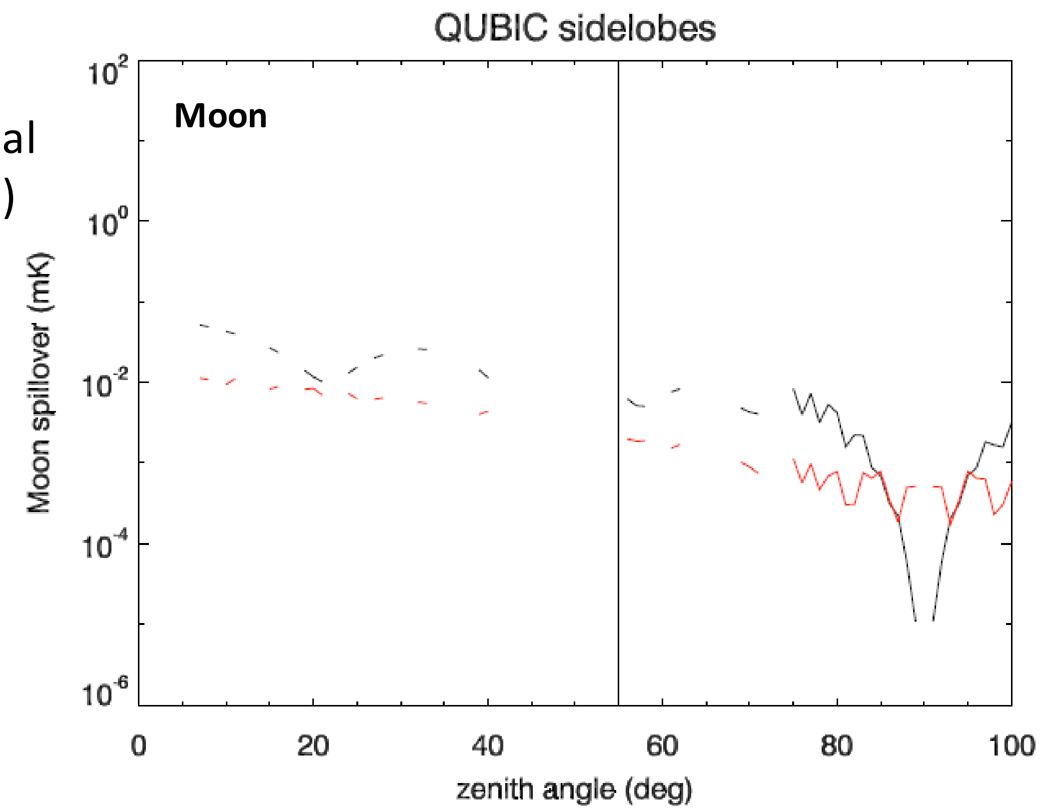

# QUBIC Spillover

Same analysis has been conducted considering the presence of the Ground Shield (see slide 25).
The GS presence more reduces the spillover contributions due to the 3 main sources considered, the values obtained when QUBIC observes the Zenith are:

Ground = 2mk Sun = 7μK Moon = 0.1μK

The same analysis has been realized to estimate the spillover contribution picked-up by the central pixel on the focal plane, in this case has been assumed, as instrument pattern $AR(\vartheta, \varphi)$, the synthesized beam (see slide 18) with a cut at $\pm 9^{\circ}$ due to detector array size (no shields are included)

Ground = 44mk Sun = 147μK Moon = 3μK

**Earth**

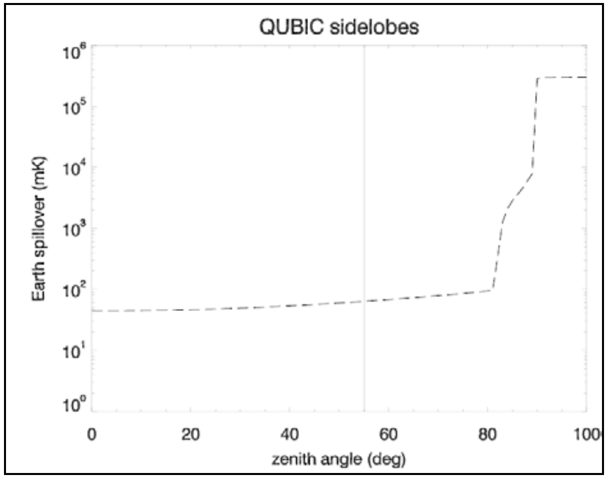


**Sun**

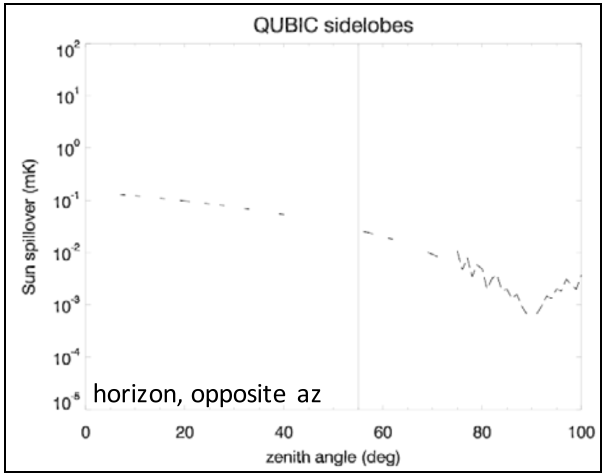


**Moon**

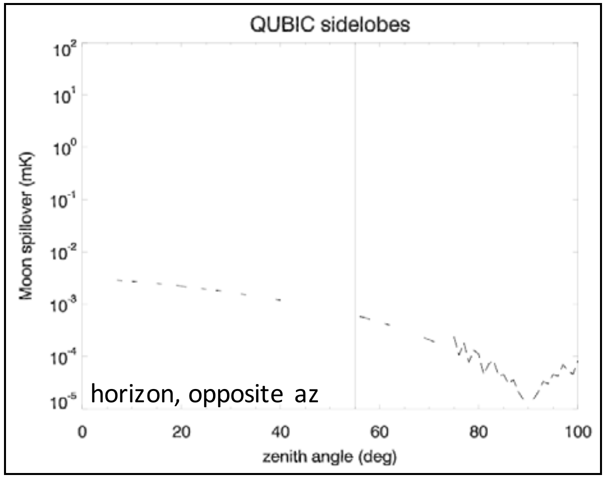

# QUBIC Spillover

To define the acceptable amount of the spillover, we keep in mind the following constrains:

- the radiative loading on the detectors focal plane coming from each feed pattern
- the faint sky signal (in terms of temperature) that will be detect

Necessity to analyze different geometries for the FB and the GS to reduce as much as possible spillover contaminations (including also the possibility to realize the Elizabethan Collar)

# QUBIC Atmo

✓ To correctly select the right number and the best geometry for the shields realization is necessary to put attention on treatment of the radiative loading incoming on the pixels of the focal plane given by the atmosphere, and to compare it with the ground pick-up

The radiative loading (in terms of power) coming from atmosphere, varying the pointing direction, can be expressed in the following way

$$P_{atmo}(z) = \frac{1}{2}\Delta\nu A_h N_h t_{tot}\epsilon_{opt}\int_{\Delta\theta}\int_{\Delta\phi} GB(\theta,\phi)B(\theta,\phi)sin\theta d\theta d\phi$$

$z$ = zenithal angle $\Delta\nu$ = *37.5 GHz*

$A_h$ = 5.9 cm² $N_h$ = 400

$t_{tot}$ = 0.59 $\varepsilon_{tot}$ = 0.2

$$GB(\vartheta,\varphi) = BB(T_{atmo}=240K)\varepsilon(z,pwv)$$ **Atmospheric Brightness**

$$\varepsilon(z,pwv) = 1 - e^{-\tau_0(pwv,\Delta\nu)\sec(z)}$$ **Atmosferic Emissivity**

**Opacity**

$$\tau_0(pwv,\Delta\nu) = (a_0 + a_1\Delta\nu/\nu) + (b_0 + b_1\Delta\nu/\nu)pwv^{(*)}$$

(*) De Gregori et al. MNRAS 2012

**Opacity *vs* Precipitable Water Vapour (*pwv*)**

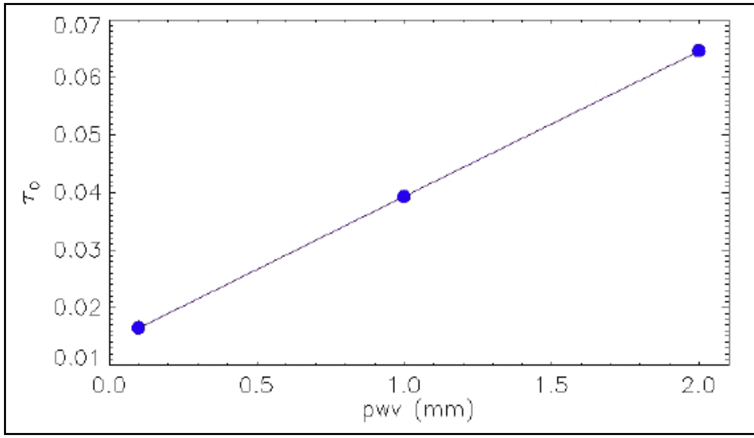

# QUBIC Atmo

$$P_{atmo}(z) = \frac{1}{2}\Delta\nu A_h N_h t_{tot}\epsilon_{opt}\int_{\Delta\theta}\int_{\Delta\phi} GB(\theta,\phi)B(\theta,\phi)sin\theta d\theta d\phi$$

Radial profile of the central pixel synthesized beam pattern (no shields) over-plotted on primary beam pattern

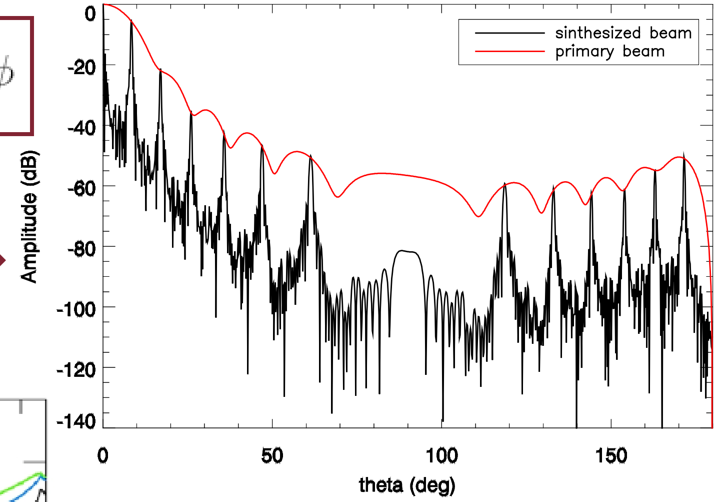


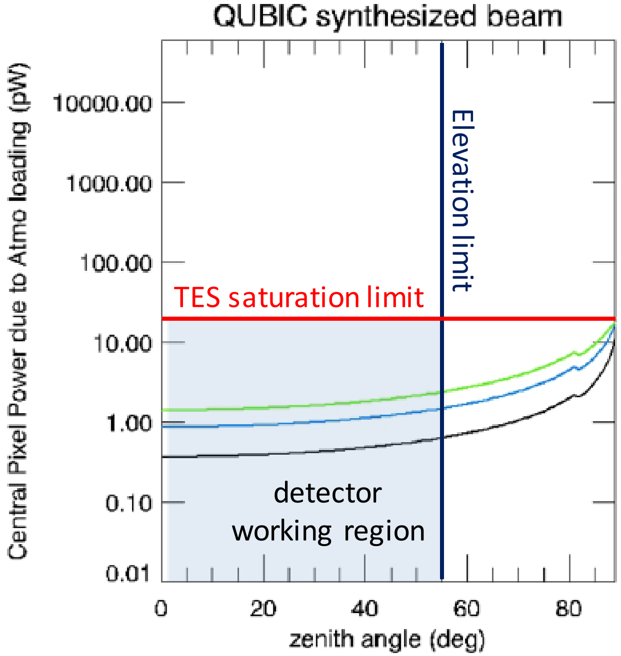


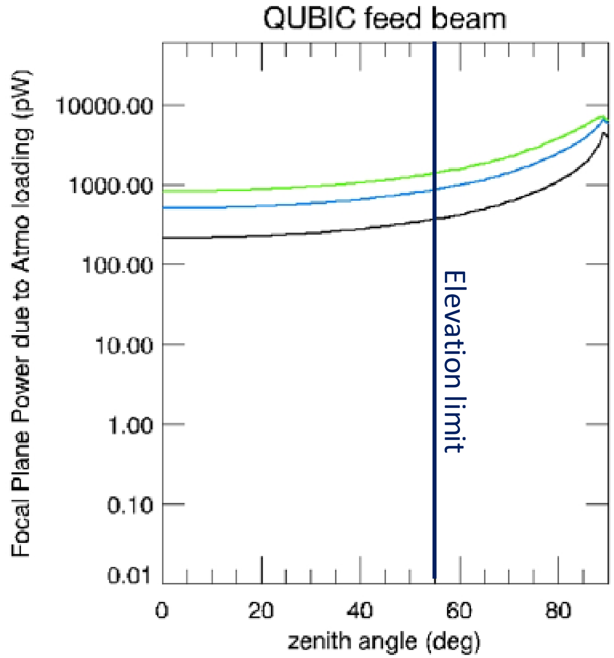


**Left Plot:** Power collected by central pixel from atmosphere for different *pwv* values ➡ $B(\theta,\varphi) = B_{synt}(\theta,\varphi)$

**Right Plot:** Total power collected by entire focal plane from atmosphere for different *pwv* values with all open feeds ➡ $B(\theta,\varphi) = B_{prim}(\theta,\varphi)$

# QUBIC Atmo

$$P_{atmo}(z) = \frac{1}{2}\Delta\nu A_h N_h t_{tot}\epsilon_{opt}\int_{\Delta\theta}\int_{\Delta\phi} GB(\theta,\phi)B(\theta,\phi)sin\theta d\theta d\phi$$

Radial profile of primary feed horn beam pattern with (red line) and without (black line) the ForeBaffle (FB)

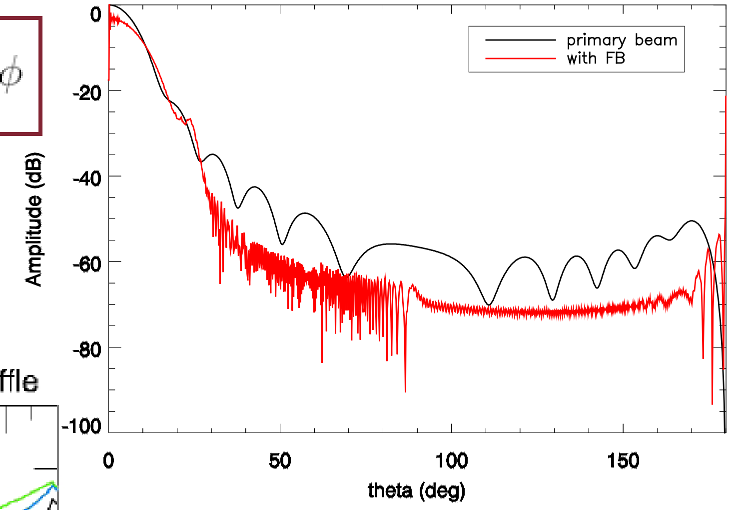


**FB geometry**: 0.5m height, aperture angle 14° , reflective inner surface

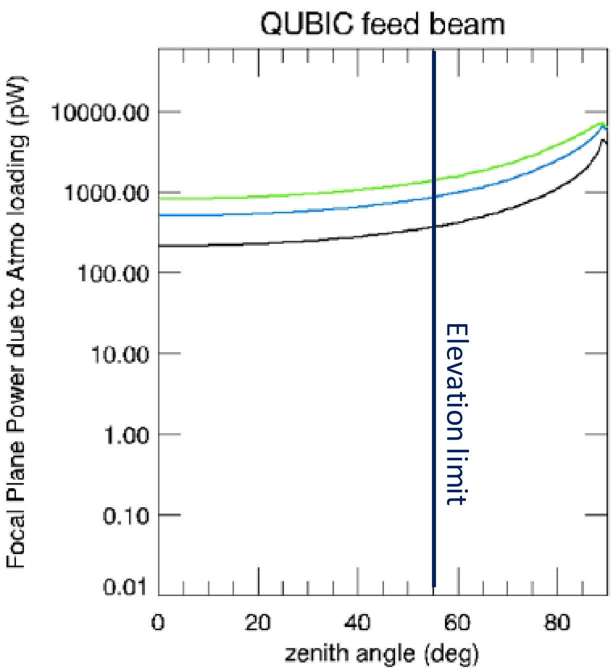


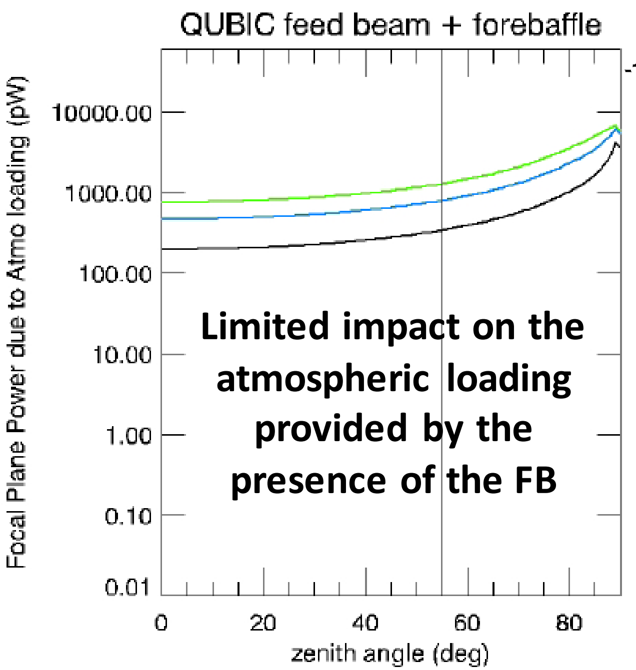


**Left Plot:** Total power collected by entire focal plane from atmosphere for different *pwv* values with all open feeds (primary horn feed pattern)

**Right Plot:** Total power collected by entire focal plane from atmosphere for different *pwv* values with all open feeds assuming the feed pattern with the FB

# QUBIC Atmo

Earth power loading → 2nd instrument sidelobes contribution for QUBIC ($T_{earth}$=270$K$ $\varepsilon$ =1 conservative approach)

Power collected on the focal plane, due to the Earth loading, varying QUBIC elevation without (left plot) and with (right plot) the presence of the FB

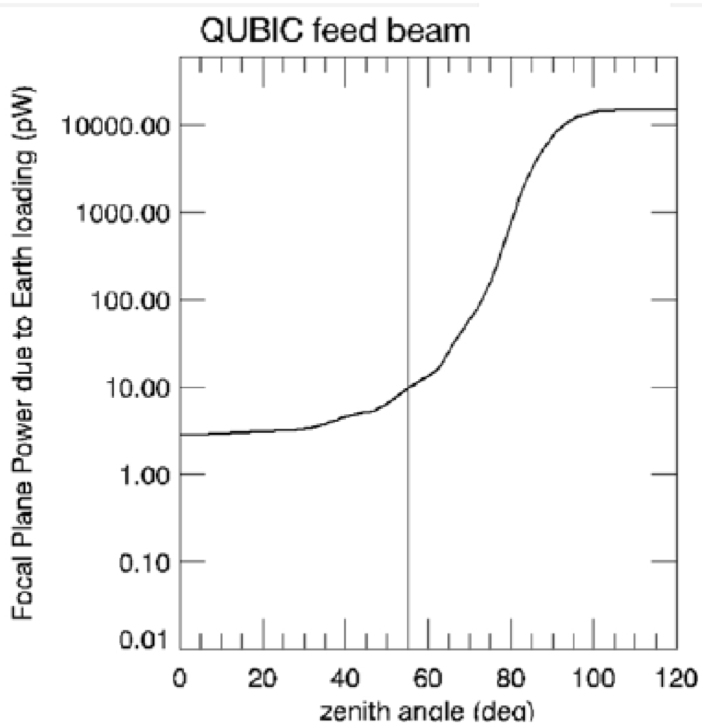


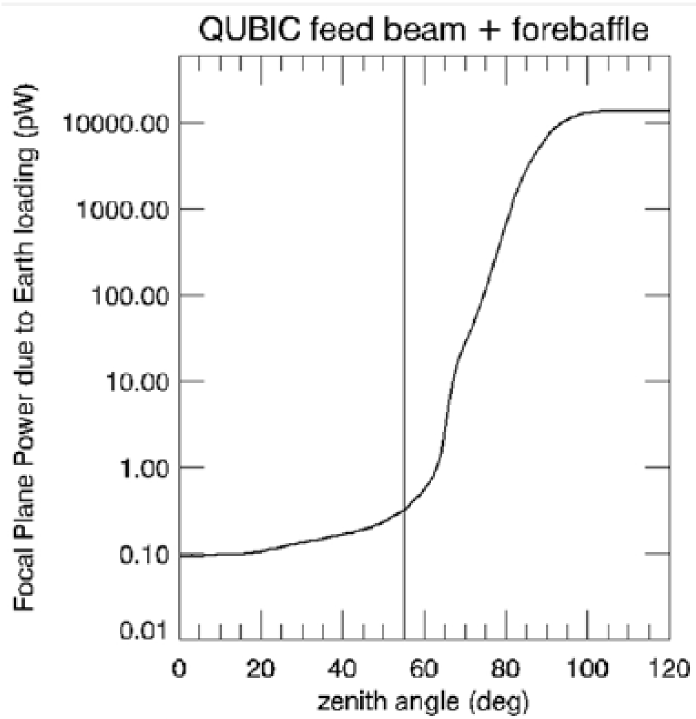


Earth's spillovers contribution is always lower than 4 pW for all the QUBIC pointing position ($N_{\text{pixel}}$=992)

# QUBIC Atmo

Power collected by the central pixel considering both unwonted sources, Atmosphere and Earth

The Atmosphere emission has the major impact in the radiative loading budget

The power collected by a single pixel (the central in the analysis) is always below the expected saturation limit (20 pW TBD) for the QUBIC detectors even under the worst *pwv* conditions (2 mm)

central pixel $0.4 < P_{atmo}$ (pW) $< 1.4$ for $0.1 < pwv < 0.4$ @ zenith

The power collected by a single pixel from Earth is 4 fW (without FB) reduced to 0.1 fW including the FB

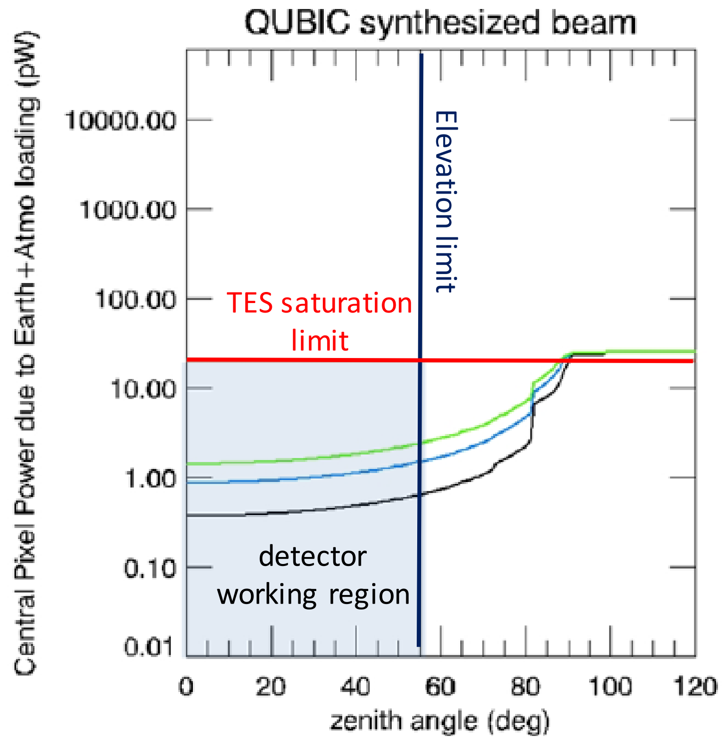


**Next steps:**

i. define the maximum acceptable loading on detectors (TES saturation limit)
ii. Realize with GRASP the synthesized beam including the presence of the shields
iii. realize a ground model emission and a model to take account atmospheric fluctuations

# Anti-Reflection Structures

The realization of optical refractive devices at millimeter and sub-millimeter wavelengths is focused to reduce the loss of the incident radiation by reflection. Fresnel reflection causes the loss of portion of the radiation incident power to be back reflected from an interface

➡ decrease of the throughput of the optical system

✓ In millimetre band is basic increase the collection of the incoming radiation especially in CMB Polarisation experiments, like QUBIC and LSPE (Large Scale Polarization Experiment), due to the small intensity of this kind of cosmological signal

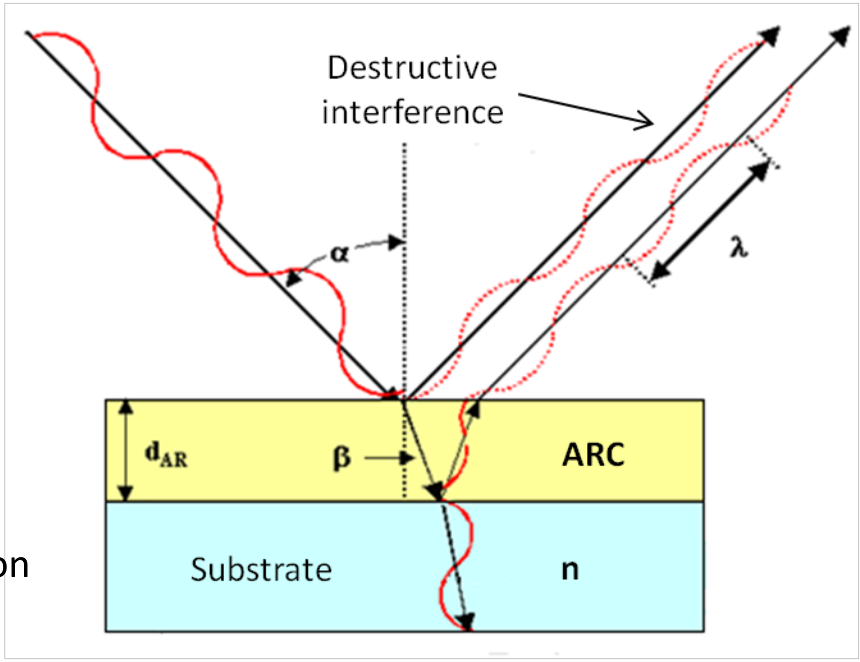


**Anti-Reflection Coating (ARC)** is the most employed technique to suppress Fresnel reflection, which consists by coating the optical element with one or more polymeric material layers or meta-materials, using the interferential behavior of the radiation inside the coating to shrink reflection

⬇

Disadvantages for mm optical devices

- thermal performances (adhesion an stability) @ cryogenic temperatures
- high realization costs

# Anti-Reflection Structures

**Anti-Reflection Structures (ARS)** is an alternative technique to reduce Fresnel reflection, originally developed for visible and infrared optical system, based on the mechanical manufacturing of the optical element surface → anti-reflection behavior due to the variation of the refractive index of the dielectric material depending on geometrical configuration of the worked surface (Priciples of Optics, Born & Wolf)

Biological inspiration → discovered by studying the geometrical shape of the cornea of night-flying moths (M. C. Hutley et al., Nature, 244, 281 ,1973)

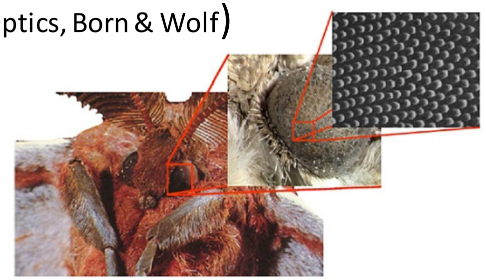

## Grating Diffraction Geometry

As a typical grating, the ARS are realized to propagate only the reflected and transmitted 0th orders (higher diffraction orders are evanescent) (Quasioptical System,P. Goldsmith)

$$n_2 \sin\theta_m - n_1 \sin\theta_i = \frac{m\lambda}{\Lambda}$$ **grating equation**

$n_2$ substrate refraction index

$n_1$ Incident medium refraction index

$\lambda$ incident free-space wavelength

$\Lambda$ grating period

$\theta_m$ angle of $m$th order

$\theta_i$ angle of incidence

$$\frac{\Lambda}{\lambda} \leq \frac{1}{\max[n_2, n_1] + n_1 \sin\theta_{max}}$$ **period to wavelength ratio**

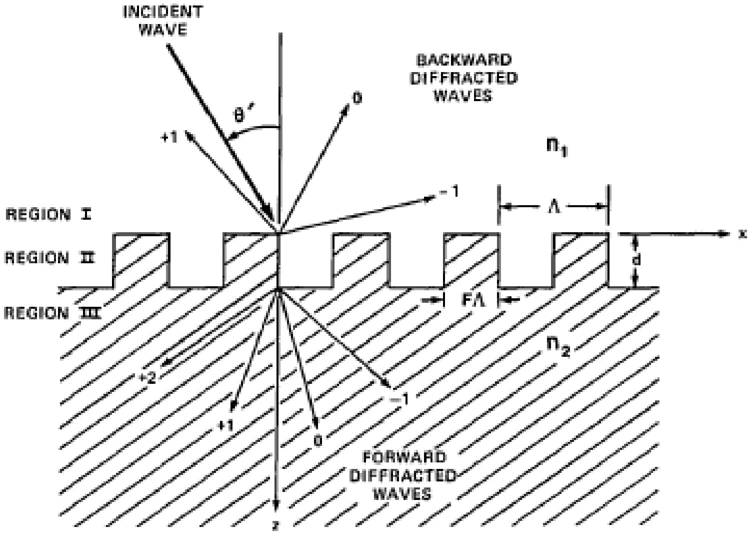

# *HFSS* Simulations

**INNOVATION** →

- Possibility to apply this kind of technique also @ mm and sub-mm wavelengths, in order to extend its application in many future astrophysical and cosmological experiments
- Low realization costs

*HFSS = High Frequency Structure Simulator* by *Ansoft Corporation vers 13.0*

analyze the electromagnetic behavior of the three-dimensional structures using the finite-elements analysis to solve the Maxwell's equations

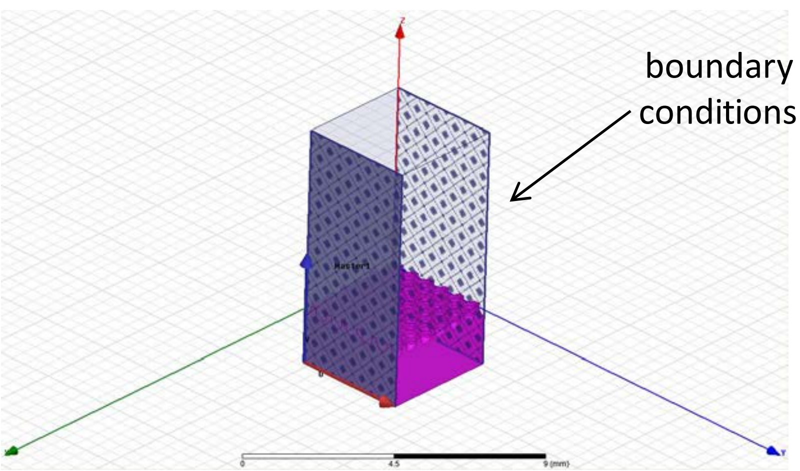


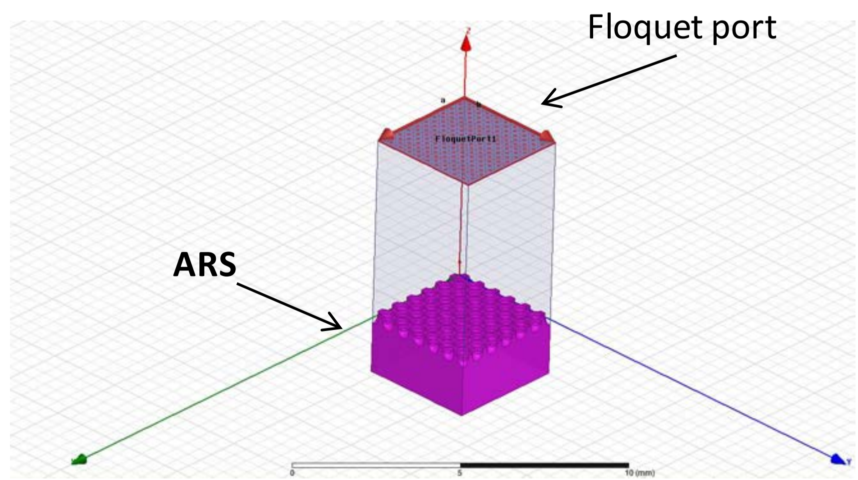

# *HFSS* Simulations Results

High Density Polyethylene (HDPE)
($n = 1.5$ $\tan\delta = 10^{-4}$)

- ✓ low absorption in the microwaves
- ✓ low cost material
- ✓ easily to work

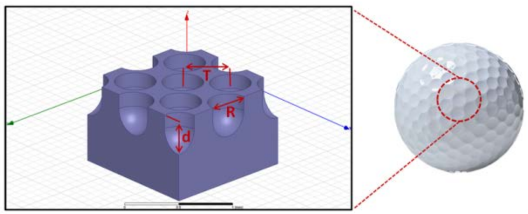


*HFSS* 3D unit cell for the single simulation performed with HFSS

**T** center to center distance between cavities
**R** radius of the cavities
**d** depth of the cavities

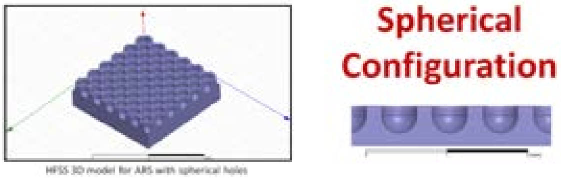

**Spherical Configuration**

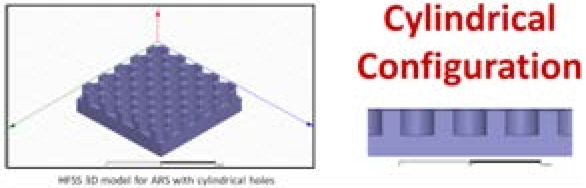

**Cylindrical Configuration**

*HFSS* simulation results relate to the two geometrical configurations analyzed (spherical and cylindrical) for different geometrical parameters

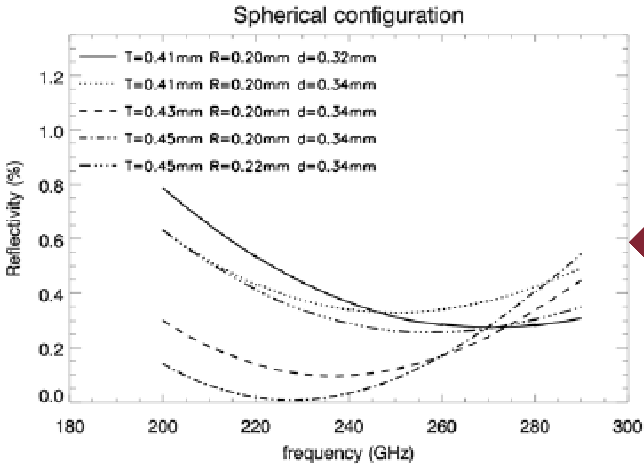


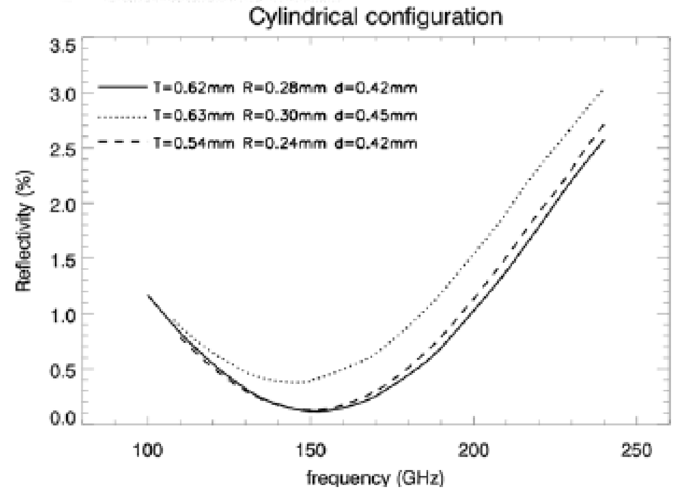

# *HFSS* Simulations Results

Reflectivity *vs* incident angle for the spherical configuration

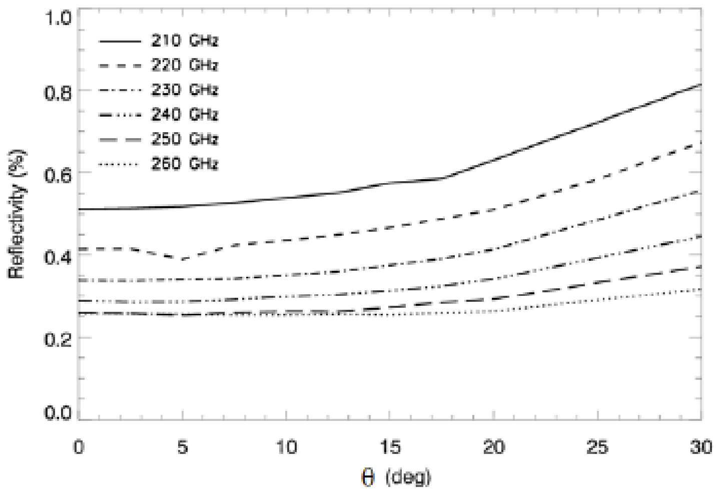


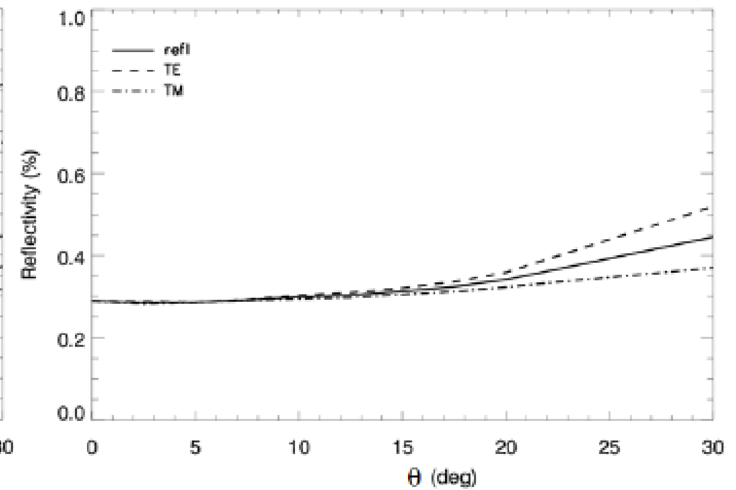


## Results from *HFSS* simulations

i. Starting from 4% reflectivity, derived by Fresnel equation for a smooth HDPE slab, the simulations show how the ARS allow to reach a reflectivity lower than 0.4%

ii. Best performance are obtained with the spherical configuration

iii. Presence of spurious polarization component (upper right plot) , manly for incident angles greater the 20° ; this effect must be taken into account concerning the use of the ARS in polarization experiments

Next step will be the realization of the first ARS prototype to realize the experimental measurements tanks to validate the results obtained by simulations

# Conclusions

- **Bolometric Interferometry:**

  a new approach for B-modes quest

- **QUBIC Experiment**

  shielding analysis with GRASP

- **Anti-Reflection Structures @ mm band**

  innovative realization technique

daniele.buzi@roma1.infn.it

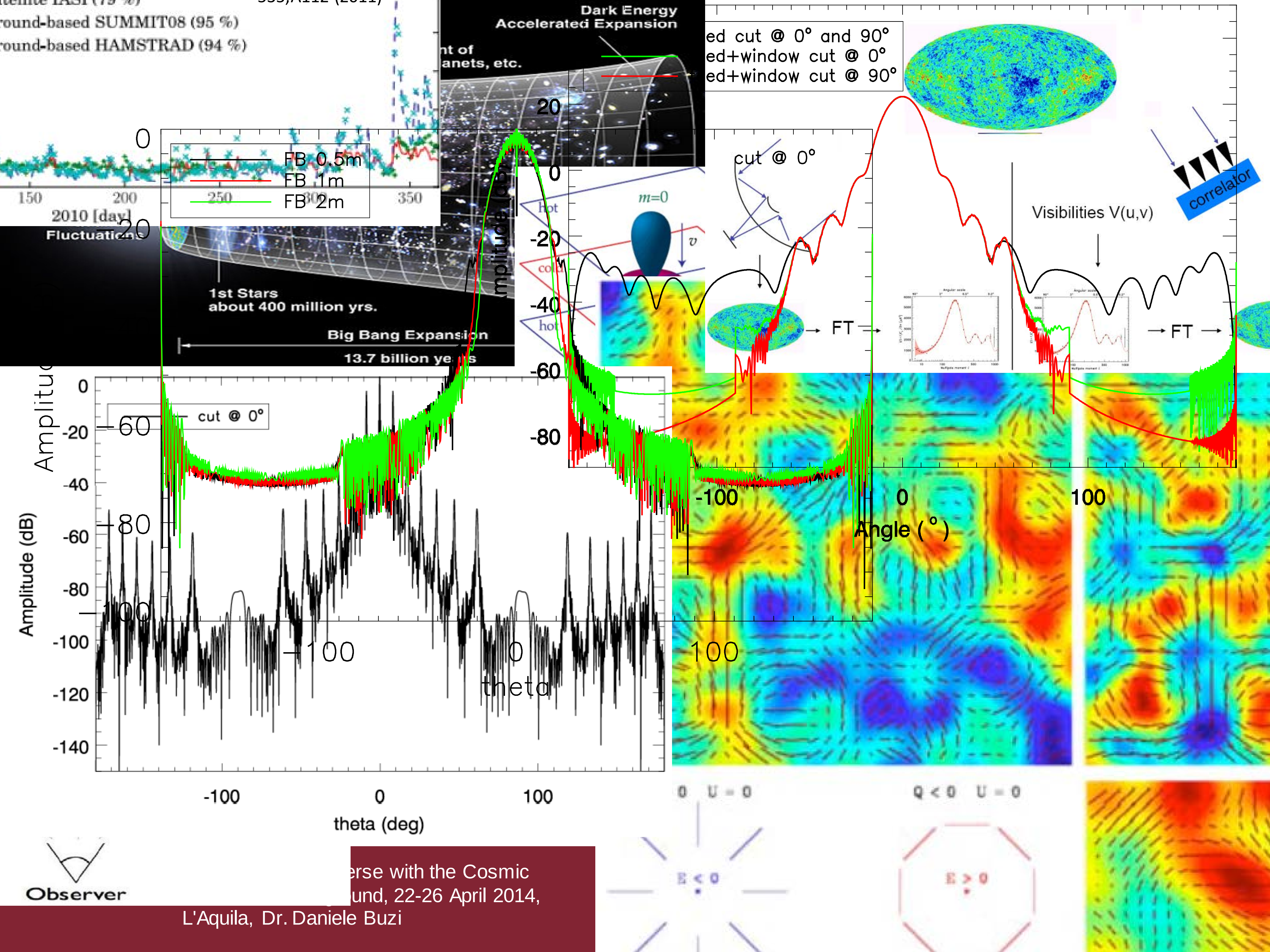

round-based SUMMIT08 (95 %)
round-based HAMSTRAD (94 %)
2010 [day]
Dark Energy
Accelerated Expansion
anets, etc.
Fluctuations
1st Stars
about 400 million yrs.
Big Bang Expansion
13.7 billion years
FB 0.5m
FB 1m
FB 2m
ed cut @ 0° and 90°
ed+window cut @ 0°
ed+window cut @ 90°
cut @ 0°
m=0
hot
cold
v
Visibilities V(u,v)
correlator
FT
Angle (°)
Amplitude (dB)
theta
theta (deg)
Q < 0 U = 0
E < 0
E > 0
Observer

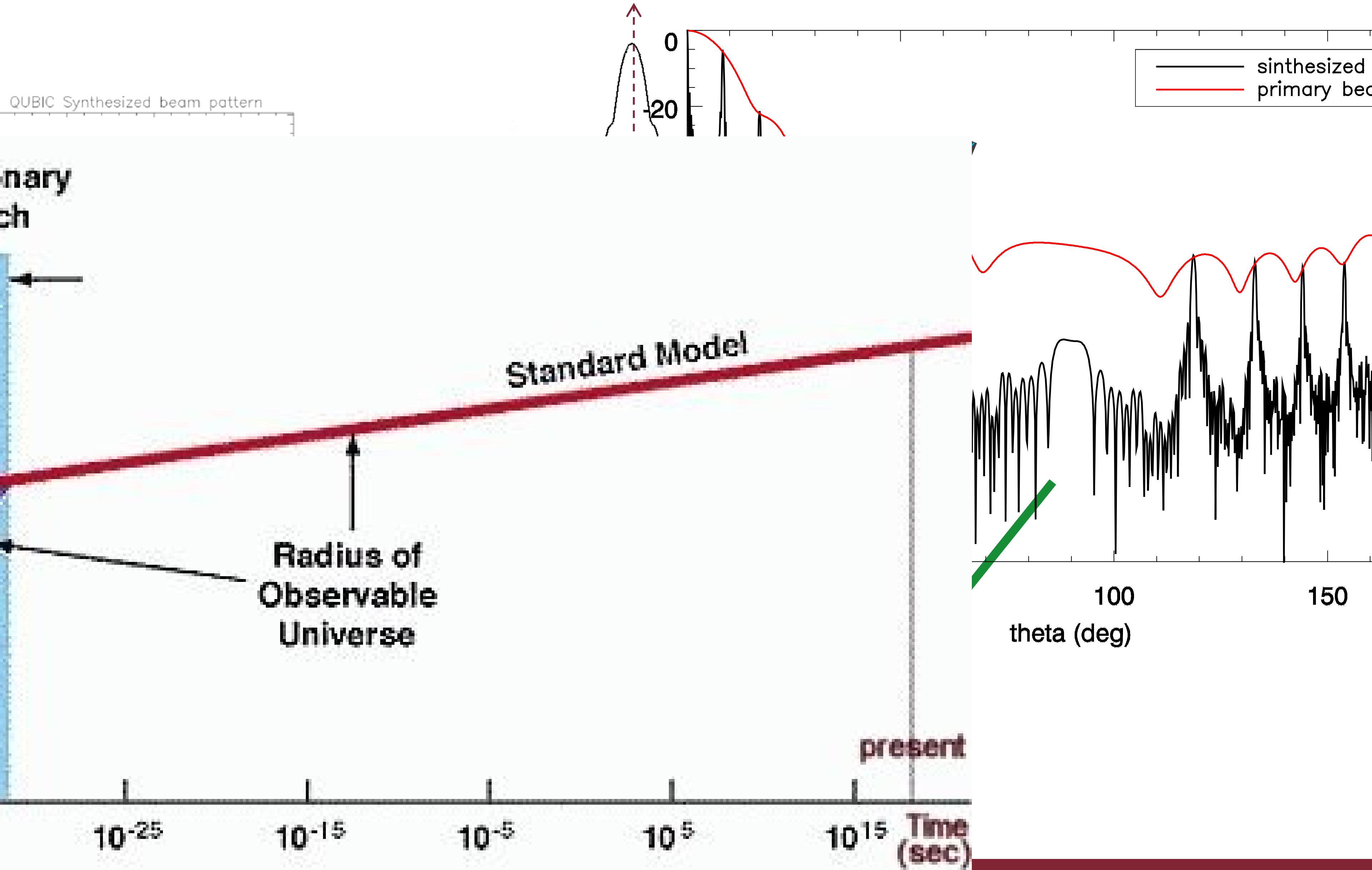
QUBIC Synthesized beam pattern
0
-20
sinthesized
primary
Standard Model
Radius of Observable Universe
present
$10^{-25}$
$10^{-15}$
$10^{-5}$
$10^{5}$
$10^{15}$
Time (sec)
100
150
theta (deg)